A Critical Review of the
Transport and Decay of
Wake Vortices in Ground Effect

rapid decay, rapid lateral motion,
intensified turbulence, flow separation, rebound *&*
more!

T. 'Sarp' Sarpkaya

Mechanical and Astronautical Engineering
Naval Postgraduate School, Monterey, CA

April 27-29, 2004

New Orleans

Now that we have proved that objects heavier than air can fly, I presume that the next greatest difficulty will be the taking off and landing of such objects.

Lord Kelvin

Wake Vortex Separation Sets
the Current System Capacity Limit

"It is time to apply our considerable knowledge of wake vortex and atmospheric physics behavior and modern instrumentation to a more dynamic wake vortex separation standard."

"The standard recognizes safe runway-occupancy time as the fundamental separation criteria, with wake vortex separation added only when a wake vortex hazard exists."

Rutishauser, Danohue, Haynie (2003)

In the beginning….

We must note that any assessment of the ground effect is certain to be incomplete. There is too much that we do not know for us to give a definitive account of the subject but, as we shall see in the following slides, a great deal has also been learned in the past decade and many aspects of Wake Vortices and their interaction with each other and with the environment have been understood.

Many of the unresolved problems are related to our inability to define and quantify the environment, to our lack of understanding of the physics of the phenomenon, and to our limitations to compute the behavior of unsteady turbulent flows with sufficient accuracy.

Most of our current understanding comes from field experiments, Large Eddy Simulations, a handful of laboratory experiments, and a few fundamental studies of the physics of the stability of vortices and vortex pairs.

Molding all this into

A physics-based parametric model for the prediction of
(operational) real-time response constitutes the essence of the problem.

VORTEX - BODY ENCOUNTER

◆   The encounter of a vortex with a solid body is always a complex event involving turbulence enhancement, unsteadiness, and very large gradients of velocity and pressure.

◆   Wake encounter IGE is the most dangerous of them all. Interaction of diverging, area-varying, and decaying aircraft wake vortices with the ground is very complex because both the vortices and the flow field generated by them are altered to accommodate the presence of the ground (where there is very little room to maneuver) and the background turbulent flow.

When are the Vortices IGE?

- The answer is somewhat arbitrary because the vortices "feel" the presence of the ground the moment they are created.

- However, assuming ideal vortices of equal strength and no wind/shear, one can calculate when a chosen quantity will differ more than (say) 1% due to the presence of the ground (conceptually similar to the definition of a BL thickness). One may use the relative height at which u component or the v component of velocity, or the ratio u/v, or lateral spacing will change by 1% or more % relative to the NO IGE case. Such calculations show that:

- (a) the (parallel) ideal vortices do not come closer than a distance of $b_o/2$ to the runway and they 'feel' the ground at about $z \approx 2\ b_o$. This is rather approximate because the real vortices decay, have finite r_o, their shape is not circular, they are affected by wind-shear, and ambient turbulence, etc.

The velocities may be calculated anywhere in the flow field from

$$u - iv = dw/dz \qquad (3)$$

Of particular interest are the velocities on the free surface and at the center of a vortex. Evaluating Eq. (3) through the use of Eq. (2) and setting y = v = o, one has[15]

$$\frac{u_s}{V_o} = \frac{2\eta_v}{(\xi - \xi_v)^2 + (\eta_v)^2} - \frac{2\eta_v}{(\xi + \xi_v)^2 + (\eta_v)^2} \qquad (4)$$

where u_s is the velocity at the free surface.

The velocity components at the center of a vortex may be obtained from Eq. (3) by omitting the contribution of the vortex itself to the velocity at its center. This procedure yields[15],

$$\frac{u_v}{V_o} = \frac{(\xi_v)^2}{2\eta_v\ [(\xi_v)^2 + (\eta_v)^2]} \qquad (5)$$

$$\frac{v_v}{V_o} = \frac{-(\eta_v)^2}{2\xi_v\ [(\xi_v)^2 + (\eta_v)^2]} \qquad (6)$$

The trajectories of the ideal line vortices approaching a rigid plane are hyperbolas given by[17],

$$(\xi_v)^{-2} + (\eta_v)^{-2} = 4 + \Delta^{-2} \qquad (7)$$

The vortices do not come to the plane surface a distance closer than

$$\eta_{min} = y_{min}/b_o = [4 + \Delta^{-2}]^{-1/2} \qquad (8)$$

O U T L I N E _of the_ P R E S E N T A T I O N

* Some general comments

* Vortex Models

* Vortices , Runways & Environment

* Wake Vortex Decay Mechanisms

* Time Evolution within IGE

* Crosswind/shear & Trajectories

* Mechanisms of Rebound

* Prediction of Ground Effects

* Brief summaries of earlier contributions

* Detailed discussion of recent contributions

* Laminar Flow IGE studies

* Shedding of Secondary Vortices

* Interaction of BL and Vortex

* Algorithms that mimic the Ground Effect

* "VORTEX"

* On Numerical Simulations

* 3-D LES (Proctor et al.)

* P2P (Holzäpfel, et al.)

* Vortex Element Methods

* SABIGO's analysis

* Integral-Momentum for Unsteady BLs

* Vortex Decay IGE

* Summary

Vortex Models

- A number of vortex models have been cited in the literature. Apparently, some of the previous references have been overlooked. For example, the model attributed to Hallock-Burnham has been first devised by L. Rosenhead in 1930 in a seminal paper.

- Subsequently, Rosenhead's equation appeared in numerous Fluid Mechanics journals and Books, but apparently has not yet entered into the literature dealing with aircraft wake vortices.

We propose that this be corrected.

More on Lamb & Rosenhead on the next slide!

Rankine vortex

$$v_\theta(r) = \frac{\Gamma_0}{2\pi r_c} \frac{r}{r_c} \quad \text{for } r \leqslant r_c,$$

$$v_\theta(r) = \frac{\Gamma_0}{2\pi r} \quad \text{for } r > r_c.$$

Lamb–Oseen vortex

$$v_\theta(r) = \frac{\Gamma_0}{2\pi r}\{1 - \exp(-1.2526(r/r_c)^2)\}.$$

Hallock–Burnham vortex

$$v_\theta(r) = \frac{\Gamma_0}{2\pi r} \frac{r^2}{r^2 + r_c^2} \quad \textit{Rosenhead (1930)}$$

Adapted vortex (Proctor)

$$v_\theta(r) = 1.4 \frac{\Gamma_0}{2\pi r}\{1 - \exp(-10(r_c/B)^{0.75})\}$$
$$\times \{1 - \exp(-1.2526(r/r_c)^2)\} \quad \text{for } r \leqslant r_c,$$

$$v_\theta(r) = \frac{\Gamma_0}{2\pi r}\{1 - \exp(-10(r/B)^{0.75})\} \quad \text{for } r > r_c.$$

Vortex Models: Rosenhead, Lamb & Hybrids

L. ROSENHEAD's (1930) Vortex Model

Vortex Element Methods for Flow Simulation

he called "an artificial smoothing parameter" to obtain

$$u_k - iv_k = \bar{z}_k = \frac{1}{2i\pi} \sum_j \frac{\Gamma_j}{z_k - z_j} \frac{|z_k - z_j|^2}{|z_k - z_j|^2 + \delta^2}. \qquad (2.42)$$

Equation (2.42) is identical to Meng's (1978) modification of (2.40b) to include a core radius as

$$u_k - iv_k = \bar{z}_k = \frac{1}{2i\pi} \sum_j \Gamma_j \frac{z_k - z_j}{r_{jk}^2 + r_c^2}, \qquad (2.43)$$

which in turn is the two-dimensional version of the desingularization scheme proposed by Rosenhead (1930).

The use of an Oseen or Lamb vortex to simulate an expanding vortex core is not identical to the use of Rosenhead's smoothing scheme. The two methods yield nearly the same tangential velocity distributions as a function of r/δ for $1.44 < 4vt/\delta^2 < 1.63$ (see Fig. 2). The viscous-diffusion solution of Lamb for an isolated line vortex corresponds to an ever-increasing δ in (2.42) for $4vt/\delta^2 > 1.63$. For this reason, Rosenhead's scheme (δ = constant) leads to the roll-up of tighter spirals, relative to other schemes using either the Lamb model or the Fink and Soh model (1974, 1978) (rediscretization plus a growing central line vortex).
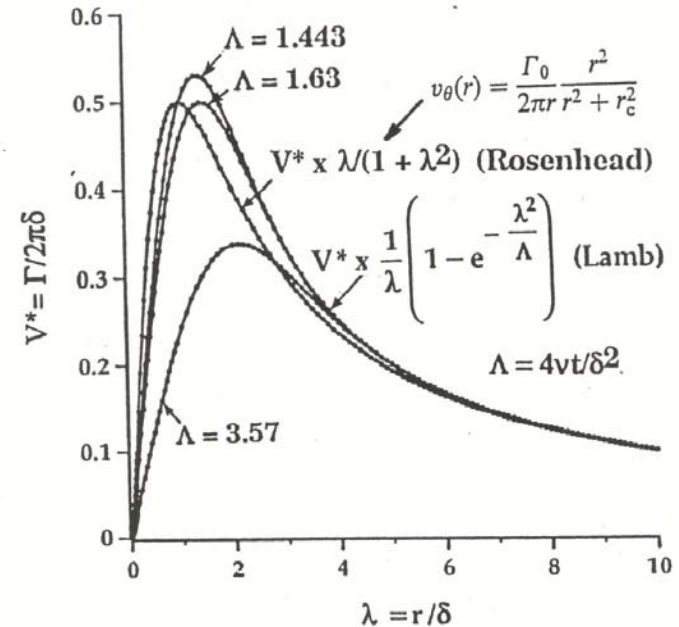
Comparison of the Lamb and Rosenhead (1930) velocity profiles

Vortices, Runways & Environment
BL Separation & Rebound
give rise to very complex experimental and numerical problems

- In general, diffusion and decay depend on a number of parameters [turbulence intensity, integral length scales of turbulence [(λ_x, λ_y, λ_z, λ_t), λ_x (along the runway) being the most important], co-operative instability mechanisms (e.g., Crow & linking), stratification, the ground effect, crosswind/shear and other physical and environmental conditions such as buildings and trees]. The parameter r_{core}/b_o has no significant effect.

- Vortices deform and decay primarily due to the overlapping of oppositely-signed vorticity (brought about by vorticity stretching and azimuthal structures). The role of turbulence is very strong on two accounts:
  (i) the BL separation and rebound are delayed because the turbulent BLs resist separation better; and,
  (ii) the rebound is limited (in relative height and number) because the vortices are strongly dissipated.

- Numerical simulations at high Reynolds numbers (Re $\approx 10^5 \Rightarrow 10^7$, with constant viscosity & no real turbulence, using either N.-S. Eqs., or Discrete Vortex Models) do not shed any physical insight.

10

Wake Vortex Decay Mechanisms in the Atmosphere
F. Holzäpfel, et al., Aerosp. Sci.& Technol., 2003

Figures (left) show the Iso-surfaces of lateral and vertical vorticity components for two N values.
"The turbulent decay of trailing vortex pairs in stably stratified environments," (F. Holzäpfel, T. Gerz,
R. Baumann, Aerosp. Sci.& Technol., 2001).
Figures (right) show the top and side views of the iso-surfaces of all three vorticity components.
Note the vorticity transport across the symmetry plane in the top view, as noted by HGB.
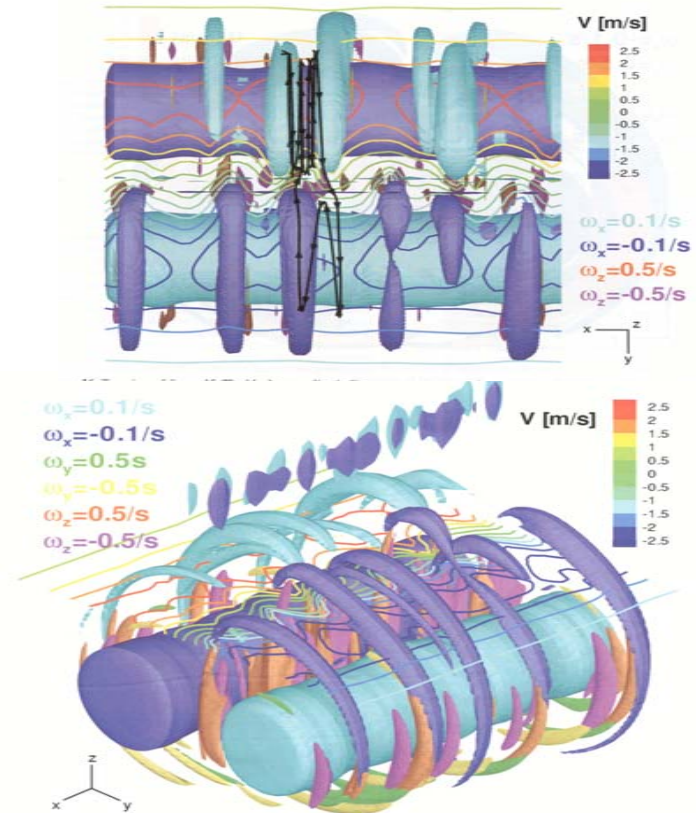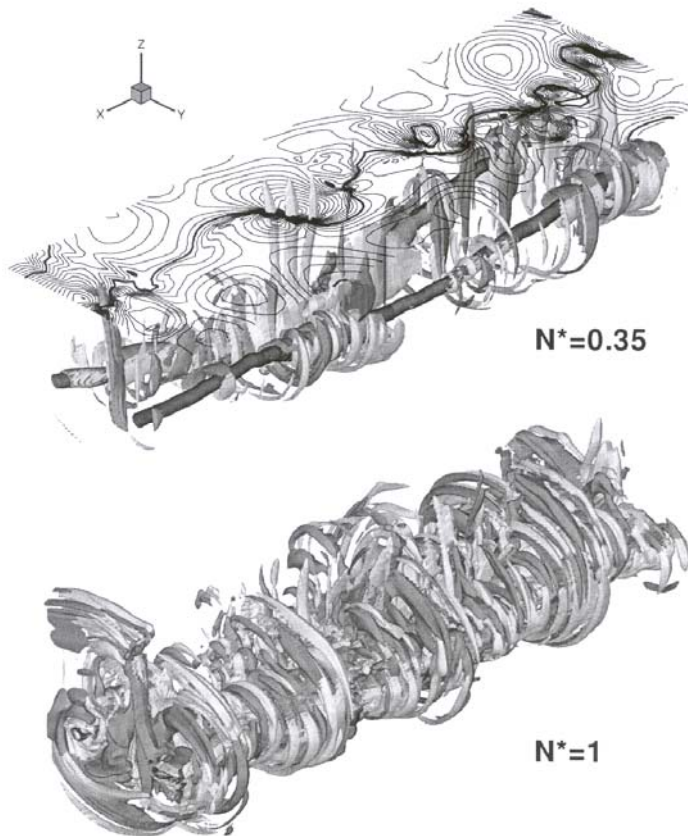
Time Evolution within IGE of a Wake Vortex Pair
(Proctor, Hamilton, Han, AIAA 2000-0757)
The figures show the top and side views of the time evolution of a vortex pair
IGE
for two different rates of dissipation
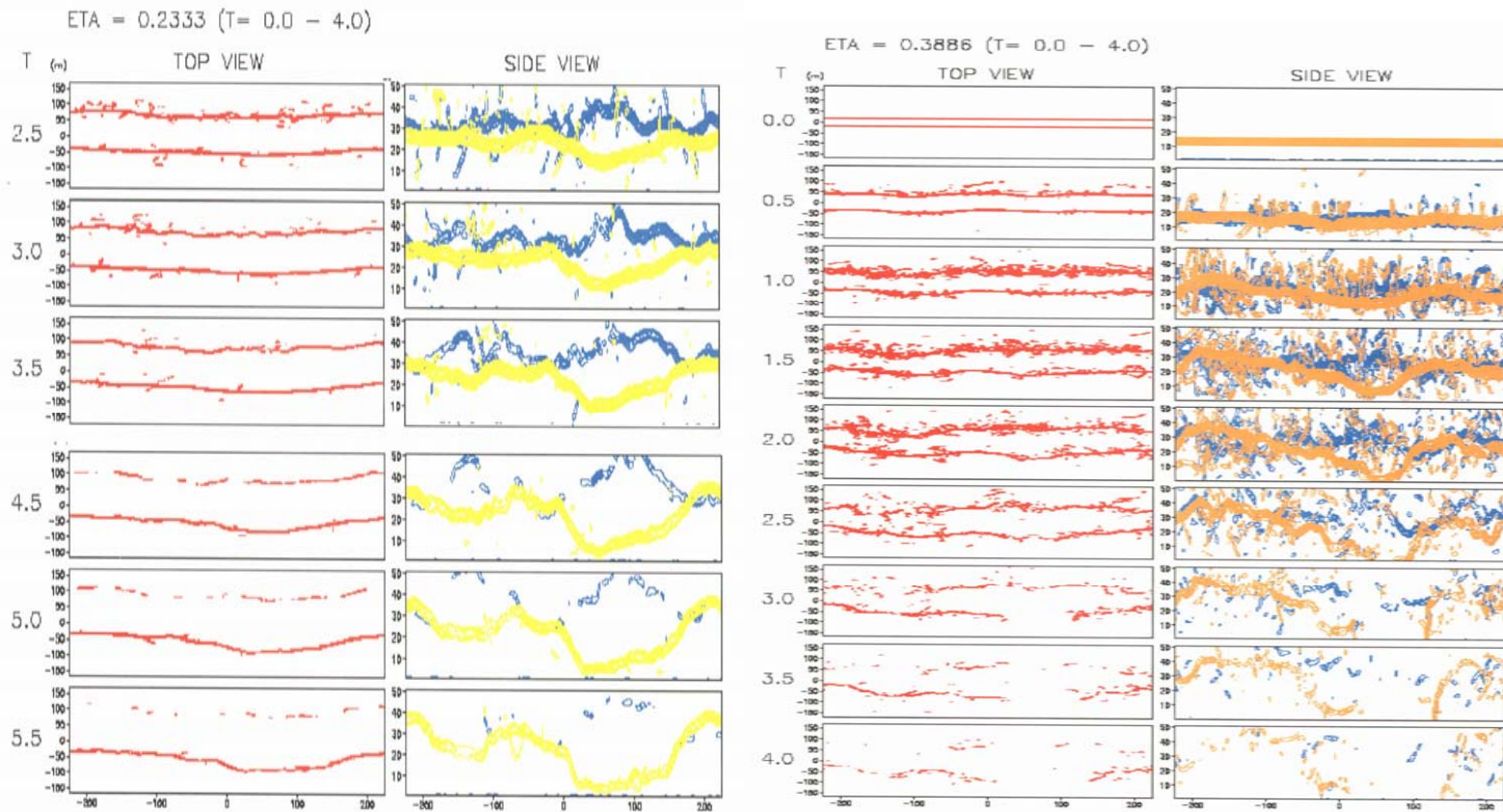(to be discussed in more detail later)

ETA = 0.2333 (T= 0.0 − 4.0)

ETA = 0.3886 (T= 0.0 − 4.0)

Figure 8. *Same as Fig. 7, but for η = 0.233.*

igure 7. *Time evolution within IGE of wake vortex pair for η = 0.388. Top (x,y) and side (x,z) view of wake vortices at increments 0.5 nondimensional time units.*

Crosswind/shear and Trajectories

• Crosswind/shear can modify the trajectories of vortices, cause lateral drift, and precipitate their degeneration, leading to non-parallel rebound, vortex tilting, unequal decay of port/starboard vortices (even leaving only a single vortex!). For single runways, cross wind is the most desirable atmospheric occurrence to have the vortices blown away from the landing path. But it is not controllable.

• The foregoing suggests that we define additional safety parameters such as $S_{pt}(z)$ to be evaluated along z (vertical distance measured from the start of the descent). They will determine the lateral positions of the port and starboard vortices as a function of z (time) and serve as a measure of safety for the following aircraft.

• It is primarily the shear and the omni-directionality of the z-dependent wind that causes the difference between the port and starboard vortices.

$$SP_{pt}(z) = 4\pi \frac{V_{wind}(z)}{\Gamma_{pt}(z)} \frac{b_o z}{(w_{runway} + b_o)}$$

$$SP_{sb}(z) = 4\pi \frac{V_{wind}(z)}{\Gamma_{sb}(z)} \frac{b_o z}{(w_{runway} + b_o)}$$

Mechanisms of Rebound

Boundary layer separation $\Rightarrow$ Creation of secondary vortices

(Harvey & Perry, 1971)

• Experiments and solutions based on the N.-S. equations show that the normal collision of a viscous vortex pair with a no-slip wall differs significantly from the predictions of the inviscid flow theory.

• The numerical and experimental evidence show that the evolution of the wake of an aircraft during takeoffs or landings (in the vertical b_o-zone or the IGE zone) is affected by the boundary layer induced by the approaching vortices (even in the absence of a pre-existing atmospheric B.L.), and no-slip & no-penetration conditions. The initial separation '~ b_o' between the vortices increases first due to both inviscid and viscous interactions and then stops where the boundary layer separates from the wall and gives rise to secondary vortices.
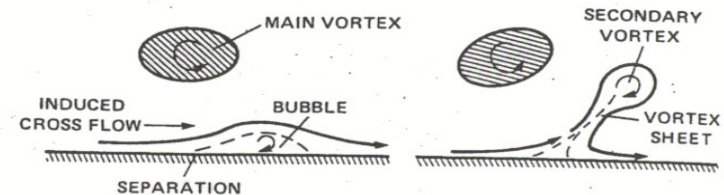
• An unsteady boundary layer forms on the ground. This is in addition to the prevailing B.L. prior to the start of the landing.

• The descent and sideways motion of the PVs give rise to strong unsteady pressure gradients along the wall ($\partial p/\partial x$) and along the z-direction ($\partial p/\partial z$), i.e., the pressure is no longer imposed on the BL as in steady flows.

• ($\partial p/\partial x$) sustains the vorticity flux into the separation region where a vorticity ligament (a nascent vortex) begins to grow.

Mechanisms of Rebound (Continued)

▪ $(\partial p / \partial z)$ sustains the vorticity flux to the top of the ligament because the pressure is highest on the on the wall and lowest at the top of the ligament. Moreover, the vorticity is lowest on the wall and highest and highest at the top of the ligament.

▪ The sign of the secondary vortices is opposite to that of the creating primary vortex.

▪ The viscous and inviscid interaction of the primary and secondary vortices and their images pushes pushes the primary as well as the secondary vortices upward.

▪ For modeling purposes, the prediction of separation points and strengths of the SVs for both the Port the Port and Starboard sides is of major importance.

▪ The measurement of the pressure [p(t)] at suitable points on the runway (in the lateral and transverse transverse directions over a large enough area) may be very informative in assessing the character and character and position of vortices, in modeling the ground effect, and in verifying the accuracy of the of the model predictions and numerical simulations.

▪ Observations made and the explanations offered regarding the generation of SVs are equally applicable to more complex cases, such as the oblique impact of a vortex ring on a plane.

Prediction of Ground Effects on Wake Vortices
Expectations and Difficulties

• The most desirable goals are the prediction of the strengths and positions of the rebound vortices in a 3-D turbulent flow (as a function of time and Re $(= \Gamma/\nu) > 10^7 - 10^8$) and the quantification of the hazard they may cause.

• The laminar-flow assumption (constant but low viscosity) to achieve a high Re is not meaningful and leads to erroneous conclusions. The decay mechanisms of the laminar and turbulent vortices are entirely different. Contrary to unwarranted claims (see, e.g., Türk, Coors & Jacon, 1999), laminar treatment at high Re does not simulate the worst case scenario. Laminar vortices spread the vorticity outward and the circulation about a contour of specified radius decreases slowly, i.e., laminar vortices decay from within through a slow diffusion. Turbulent vortices decay from the outside with minimal expansion of the core. Wind shear and ambient turbulence precipitate the onset of 3-D instabilities.
Opposite sign vorticity of the ambient crosswind decreases circulation and enhances decay of a vortex. Same sign vorticity of the ambient crosswind increases circulation and might <u>enhance or delay decay.</u>

• Three-dimensional effects caused by nonparallel cores, vortex stretching and divergence, and axial jets within the vortex core cannot be neglected particularly when linking of the vortices (with their images) are concerned. Furthermore, the role of shear on the enhancement or suppression of linking for the lower as well as higher turbulence levels needs to be explored.

Expectations and Difficulties
(continued)

Physical and numerical difficulties towards the prediction of IGE

- In laboratories, it is nearly impossible to realize long-enough moving floors, high-enough Reynolds numbers, and sufficient cross-flow and shear to simulate realistic environments;

- Carrying out numerical simulations at Re ($= \Gamma/\nu$) $> 10^7$ - 10^8 for a fully turbulent flow presents numerous difficulties and requires several simplifying assumptions.

- Numerical simulations are not focused towards an operational real-time response. They provide invaluable insight for real-time modeling.

- Physics-based and field-tested 'models' are indispensable for the real-time prediction of the behavior of vortices OGE, NGE, and IGE.

With the foregoing thoughts on mind
we will review some of the more notable contributions.

Brief summaries
of some of the earlier contributions to rebound

- Dee and Nicholas (1968) made flight measurements of wing tip vortices near the ground.

- Harvey and Perry (1971, 1977) were the first to offer an explanation for the vortex/ground interaction and the rebound.

- Barker and Crow (1977) performed lab experiments.

- Blanin et al. (1977, 1978) carried out a numerical simulation and showed rebound.

- Saffman (1979) showed that inviscid vortex pair does not give rise to rebound: they slide along the wall.

- Ciffone and Pedley (1979) made vortex trajectory and velocity measurements in the wakes of B-747 and DC-10 models IGE and reached a number of important conclusions.

- Pengel and Tetzlaff (1984) reported on wake measurements with a ground wind vortex sensing system using u-v-w anemometer.

- Orlandi (1990) performed low-Re N-S calculations with 2-D vortices and found secondary, tertiary, etc. vortices which slows down the translation of the primary vortices and forces them to rebound several times.

- Robins and Delisi (1993) made a numerical simulation of ground effect using 'a scale-dependent eddy-viscosity-like damping scheme,' no atmospheric turbulence effects, and 'a mixed no-slip/free-slip boundary condition.'

- Köpp (1994) made Lidar measurements on the parallel runways of Frankfurt/ Main and found that the vortices of one runway can reach the other after rebound.

Brief summaries
(continued)

• Kantha (1996, 1998) proposed an empirical model using <u>inviscid flow</u> and assuming that the circulation around each vortex remains unchanged. Subsequently, he introduced six empirical constants (to be determined experimentally) to simulate decay. Even if developed further, his analysis is not likely to lead to real-time predictions or to a model.

• <u>Türk, Coors, Jacob</u> (1999) used 2-D vorticity-stream-function formulation within $300 < Re < 3 \times 10^6$ (with constant viscosity, laminar flow, high Re, and No Turbulence!) and found one or more rebounds of the primary vortex pair.

In the next slide we show a list of contributions which will be discussed in greater detail.

Detailed Discussion of some contributions

- Peace and Riley (1983)
- Verzicco & Orlandi (1996)
- Manna,Verzicco & Orlandi (1995)
- Lim (1989)
- Verzicco & Orlandi (1994, 1995, 1996)
- Manna, Verzicco & Orlandi (1995)
- Corjon & Stoessel (1997)
- Puel & Victor (2000)
- Chuang & Conlisk (1989)
- Robins, Delisi & Greene (2001)
- Baren,Frech, Moet (2002)
- Proctor-Hamilton-Han (2000)

- Holzäpfel (2003)
- Holzäpfel & Robins (2004)
- Vortex Element Methods & Winckelmans & Ploumhans (1999)
- Belotserkovsky & SABIGO, Ltd. (1999)
- Loitsyanskiy (left) & Schlichting
- Wake Vortex Decay:
    J.N. Hallock (1975)
    Rudis, Burnham, Janota (1996)
    Burnham & Hallock (1998)
    Burnham, Hallock, & Greene (2002)
    Hallock, Osgood, Konopka (2003)

Laminar flow IGE

Peace and Riley (1983)

- Flow induced by a vortex pair in a viscous fluid, which is otherwise at rest, in the presence of a plane boundary. Assumptions: inviscid outer flow, no-slip boundary, and laminar flow.

- The top figure shows the contours of constant vorticity for Re = Γ/ν = 100 for various values of time. Inception of separation is clearly predicted.

- The bottom figure shows the trajectories in the flow field for Re = 100:

——— Position of maximum vorticity;
_ _ _ _ The path of a particle initially coincident with the vortex;
The inviscid trajectory: . – . – . – .
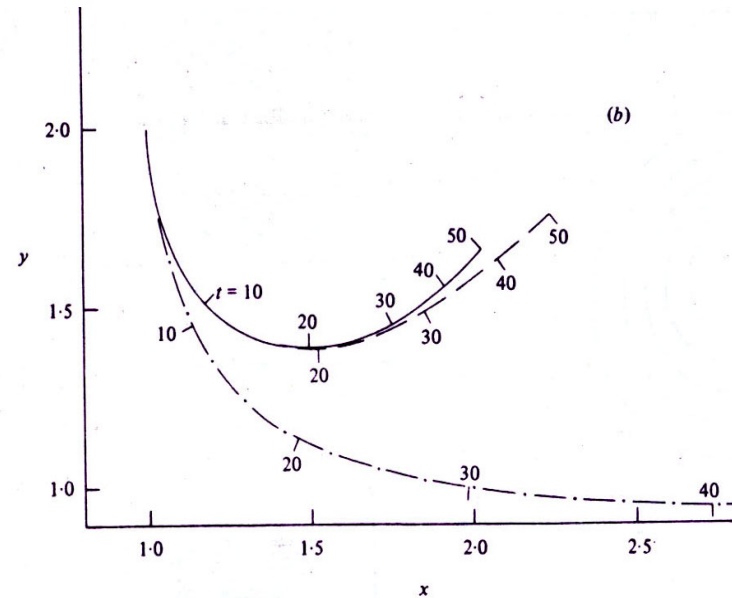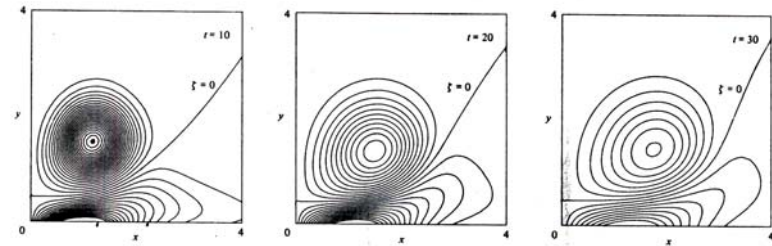
Laminar flow IGE

Zheng and Ash (1996)

- Zheng and Ash (1996) used an unsteady 2-D laminar (constant eddy viscosity) approximation of the N.-S. Eqs., to study the influence of ground coupling, stratification, and cross-wind on vortex system behavior and decay. Figure (a) shows a comparison of measured (circles) and computed (solid line) vortex trajectories and (b) the horizontal position history, all at $Re = \Gamma/\nu = 7650$.

- For the same case, Orlandi (1990) has predicted the occurrence of multiple vortex loops during similar intervals. Differences are thought to be due to the fact that "the far-field boundary conditions appear to influence trajectory over the interval of interest." Thus, the numerical and experimental boundaries may prove to be very important in such short-duration unsteady events, particularly in turbulent boundary layers.

a)

b)
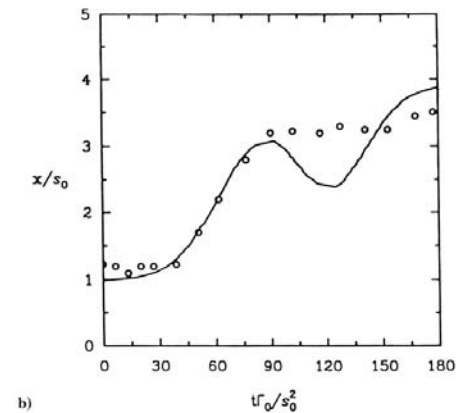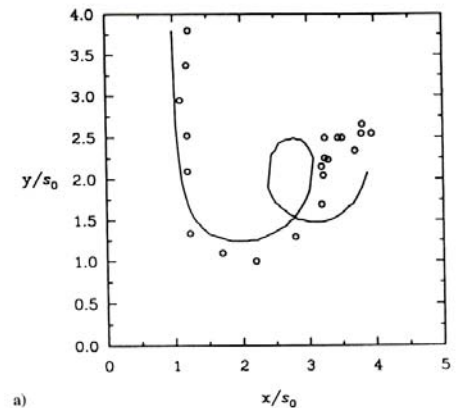
Laminar flow IGE

Zheng and Ash (1996) continued

• The figure shows the influence of the Reynolds number on vortex trajectories: (note that the flow is laminar at all Reynolds numbers because the viscosity is constant):

Re = 1,000   ....

Re = 75,000   ———

Potential flow: .─ .─ .─ .

- Figure shows the vorticity contours for a symmetric, unstratified vortex-wall encounter at Re = 75,000 for $t = \Gamma_o t/s_o^2 = $: (a) 60, (b) 120, and (c) 150.

Important facts to note are:

- Even though the secondary vortices (SVs) are weaker than the primary vortex (PV), they influence the motion of PV (as they revolve around it). At t = 60, the SV acts to retard the lateral motion of the PV. At t = 120, the SV resides directly above the PV and can strongly retard its lateral motion. At the same time a new SV is forming. At t = 150, the PV is sandwiched between two SVs.


24
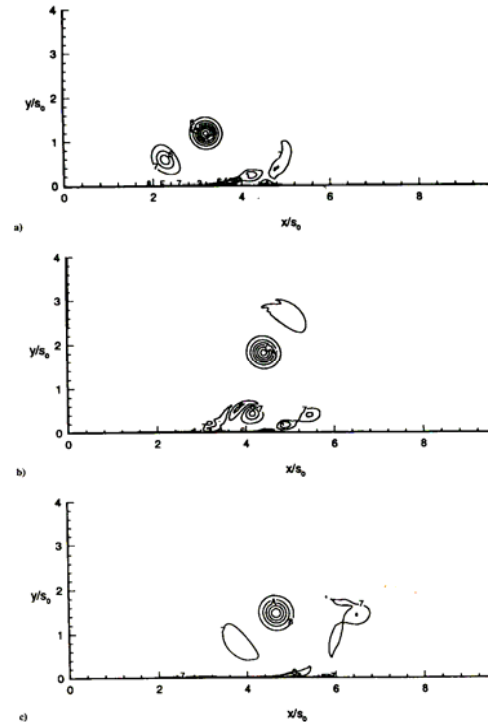
Laminar flow IGE

Zheng and Ash (1996) (Top Figure)
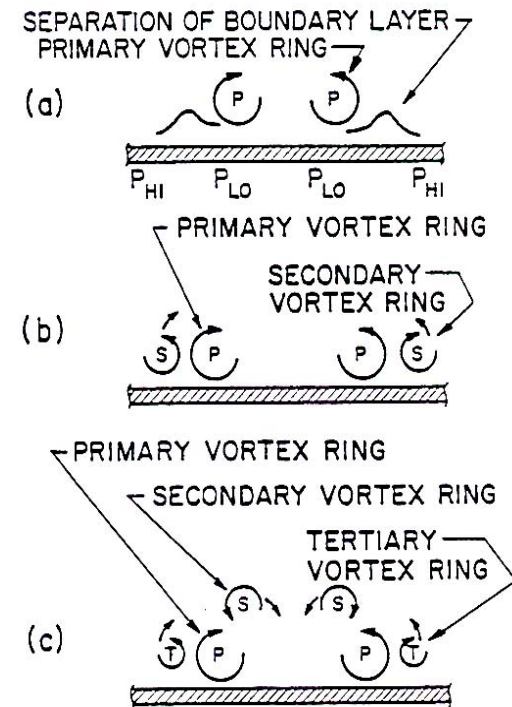Proctor (1998) (Bottom Figure)
continued

- Zheng and Ash: (Top figure)

- Vorticity contours at $\Gamma_o t/s_o^2 = 30$ for a cross-flow (from left to right) with <u>uniform shear</u> (with negative vorticity).

- The negative vorticity levels in the upwind primary vortex becomes more negative, whereas the downwind primary vortex becomes less positive (destroying symmetry!). These interact with the boundary-layer vorticity giving rise to secondary vortices and to the tilting of the vortex pair.

- Proctor: (bottom figure): Laminar vortex pair in shear and the tilting of vortices. Proctor noted that rising vortices cannot always be explained by surface rebound. Vertical shear from crosswind component can affect the descent of the vortices.
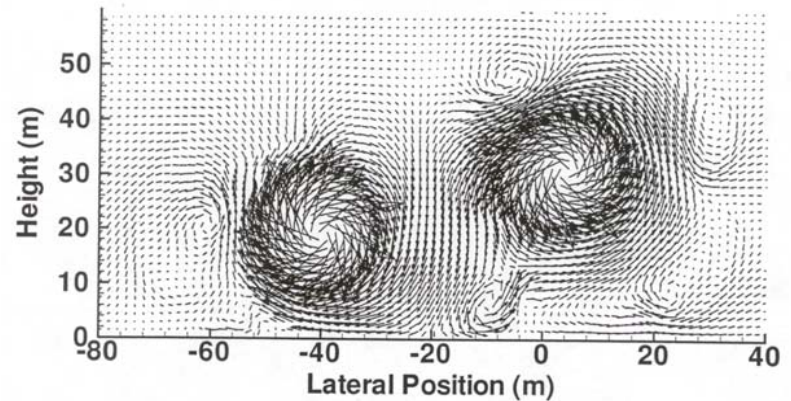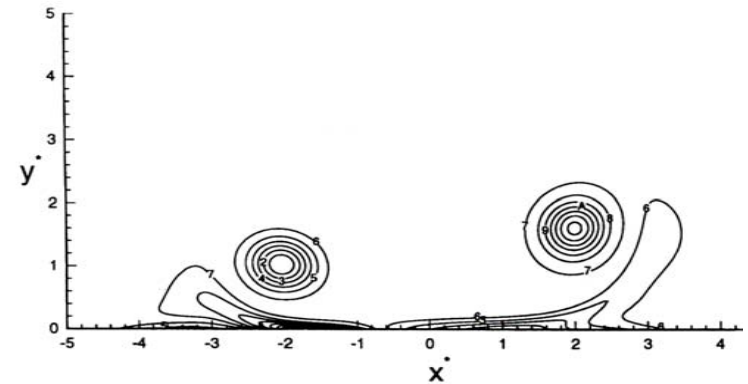
Laminar flow IGE

Verzicco & Orlandi (1996)

• Normal collision of an axisymmetric vortex ring with a wall (Cerra & Smith, 1983; Verzicco & Orlandi, 1996).

• As the ring approaches the wall and reaches a distance of about one ring radius from the wall, a thin oppositely-signed vorticity layer develops at the wall. For sufficiently large Re (=VD/ν), the B.L. separates, rolls up, and generates a secondary vortex ring. Due to mutual induction, these two rings move along a circular trajectory, and the secondary ring penetrates into the interior of the primary ring.

• If Re is large enough, the primary ring is strong enough to generate a tertiary ring. For larger Re, the secondary and tertiary rings merge to form a single structure with sufficient circulation to move away from the wall.


SEPARATION OF BOUNDARY LAYER
PRIMARY VORTEX RING

(a)

P_{HI} P_{LO} P_{LO} P_{HI}

PRIMARY VORTEX RING

SECONDARY VORTEX RING

(b)

PRIMARY VORTEX RING

SECONDARY VORTEX RING

TERTIARY VORTEX RING

(c)

Laminar flow IGE

Manna, Verzicco & Orlandi (1995)

- Normal collision of a vortex ring with a wall at
  Re = 480, (Manna *et al*., 1995).

- Left: flow visualization

- Center: numerical contour plots of a passive scalar

- Right: azimuthal vorticity plots.

  *Times are made non-dimensional using the ring
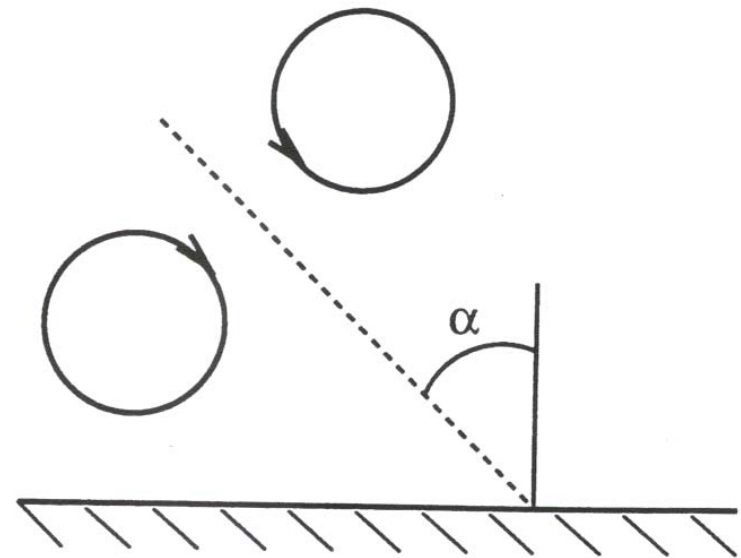 radius and its self-induced translation velocity.*

- The surface pressure generated by the (primary ring)
PR gives rise to a pushing force. The (secondary ring) SR
generates a <u>suction</u> force.
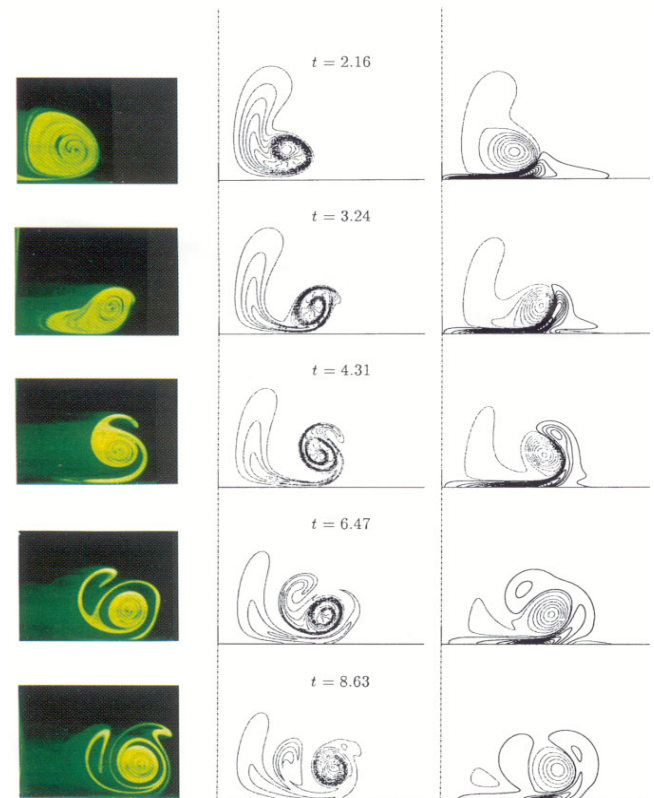
Laminar flow IGE

Lim (1989),Verzicco & Orlandi (1994, 1995, 1996)

- Sketch of the initial condition of the oblique collision of a vortex ring with a wall. Note that α = 0 is the 'normal impact.'

Laminar flow IGE

Lim (1989),Verzicco & Orlandi (1994, 1995, 1996)

- **The *wall-normal pressure gradient* drives the fluid towards the region of the ring away from the wall. This motion continuously accumulates secondary vorticity in the region where the SR is eventually ejected.** This mechanism is identical to that discussed in connection with the aircraft vortices.

- The numerical predictions, confirmed by experiments, have shown that high pressure levels are associated with the part of the ring where the vorticity is low (close to the wall) and the lower pressure levels are associated with the part of the ring where the vorticity is high.

- At high angles of impact (α) a strong axial flow is generated and the dissipation is reduced. At smaller angles, the dissipation becomes very important, as experimentally confirmed by Cerra & Smith (1983). Plots for α = 38.5 deg: Left: 2-D vortex pair; right: 3-D vortex ring, all for Re = 600.
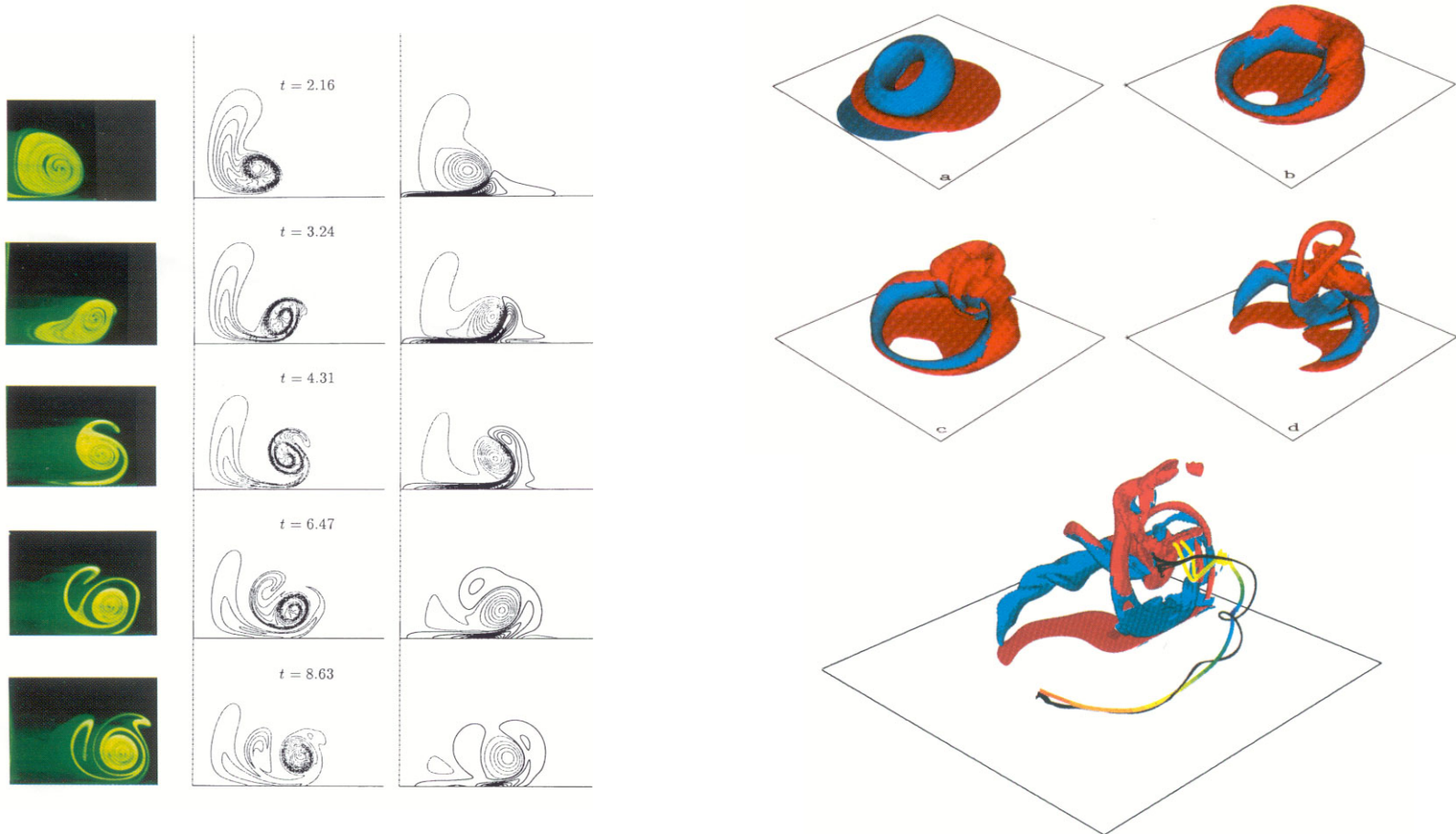

(a)
(b)
(c)
(d)

29
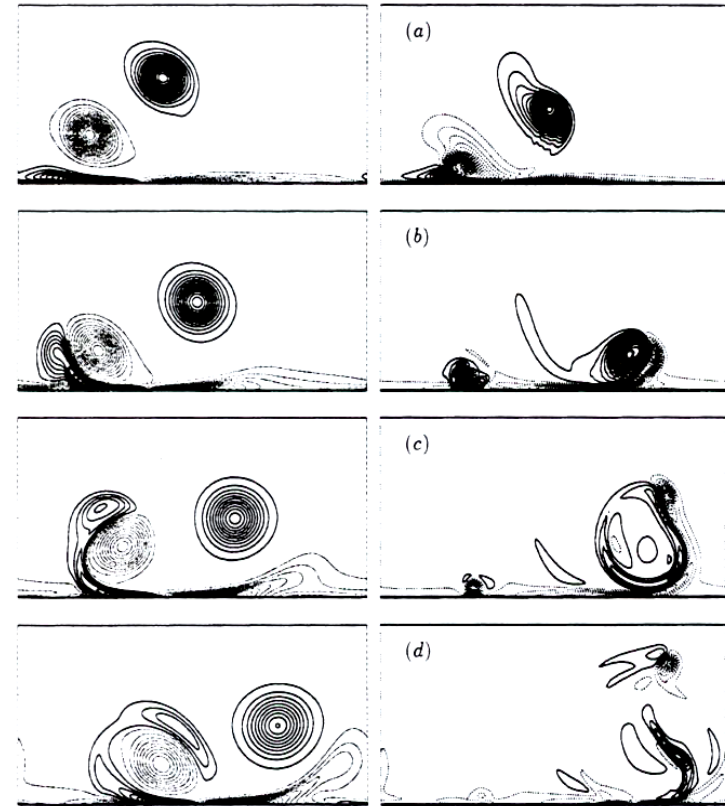
Laminar flow IGE

Manna, Verzicco & Orlandi (1995) continued
Re = 480, visualization and numerical contour plots

Normal collision   **Oblique collision**

$t = 2.16$

$t = 3.24$

$t = 4.31$

$t = 6.47$

$t = 8.63$

Laminar flow IGE

Corjon & Stoessel (1997)

- Corjon & Stoessel (1997) presented 3-D DNS (direct numerical simulations) of a pair of vortices placed in a laminar BL near the ground. Figures show the computational domain and the three-dimensional rebounding of the vortices at various times at a Reynolds number of 600.

- Corjon & Stoessel have concluded that the 2-D and 3-D rebounds are similar; the primary and the secondary vortices may reconnect, leading to the bursting of the primary vortex; and that the classical pictures of linking observed in OGE studies are not seen IGE region.

- Clearly, the Re is too small. The Re number of the IGE studies using DNS should be at least 3,000.
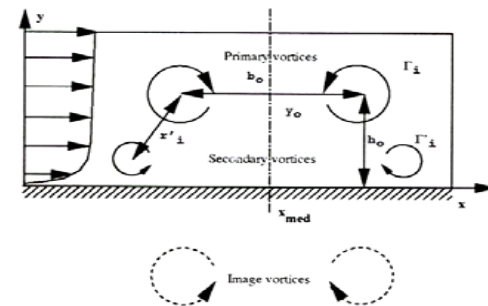

Figure 1: Computation domain

Figure 6: Three-dimensional rebound of wake vortices - t* = 0, 2.4, 4.8, 9.6 case R_1

Laminar flow IGE

Puel & Victor (2000)

- The contra-rotating vortices may induce an 'upwash' or 'fountain-upwash' effect between them at relatively small Re.

- On liquid surfaces the rebound is small and depends on the contamination and the 'roughness' of the free surface. On a clean water surface, vortex core remains compact.

- The formation of secondary vortices slows or arrests the lateral translation of the wake vortices. This leads to the looping of the main trajectories and to the generation of additional secondary vortices, (Figure from Puel & Victor, 2000). This is only so for laminar BLs and vortices.

- Turbulence and the three-dimensionality of the flow accelerate the dissipation of all vortices and strongly affect the trajectories.
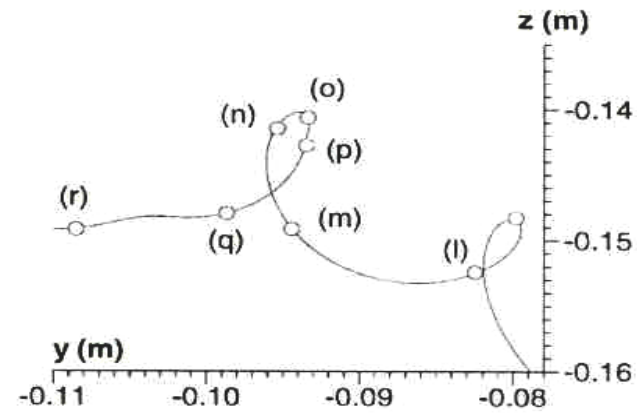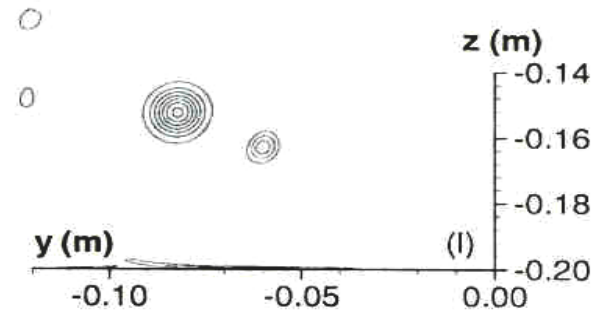
Shedding of Secondary Vortices (SVs)
## and 3-D effects

- The existing observations with <u>aircraft vortices</u> show that vortex wakes sink when out of ground effect, and tend to separate laterally and become three dimensional IGE.

- These vortices generally dissipated before carrying out multiple rebounds.

- SVs are shed in discrete quanta, <u>not as continuously rolled-up vortex sheets</u>. This is very important for modeling purposes.

- Thus, the position of the separation points, nascent strengths of the SVs, no-slip & no-penetration on the wall, a meaningful decay law, wind & shear, and stratification are the most important factors for the creation of physics-based parametric models for the prediction of (operational) real-time response.

a) unsteady 2D evolution

b) steady 3D evolution
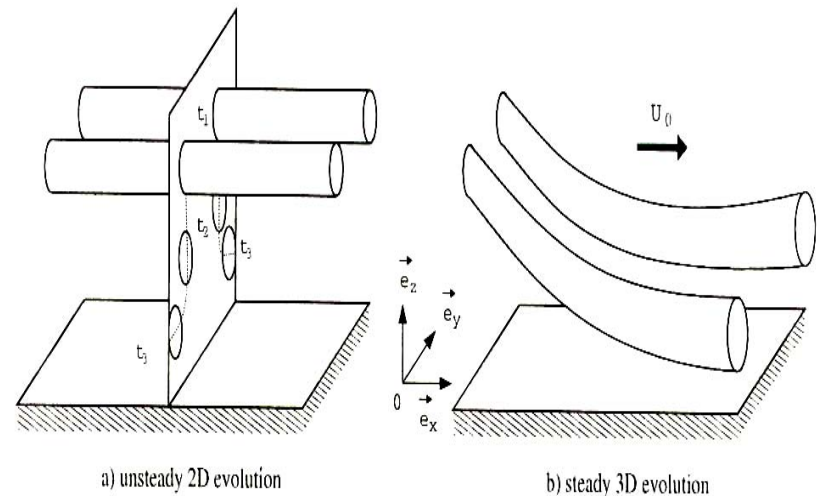
Interaction of the existing BL with a convected vortex
Chuang & Conlisk (1989)

- The figure shows the effect of interaction of the boundary layer induced by a horizontally convected rectilinear vortex in a stream of uniform velocity U (Chuang & Conlisk, 1989). The streamlines are relative to the vortex at t = 0.75 for several Reynolds numbers from Re = 8×10^3 to Re = 4.4×10^4. Re = Uh/ν where h is the elevation of the vortex from the ground. The distance h is larger than the boundary layer thickness, i.e., the vortex is initially outside the boundary layer.

- Solution is based on a combination of finite-difference methods and the Fourier-transform method, with Crank-Nicolson marching technique.

- The figure shows that the BL undergoes an unsteady separation process (the formation of a closed recirculation eddy within the BL) and, eventually, develops a kink. Computations cannot be continued further in time due to the appearance of the kink.
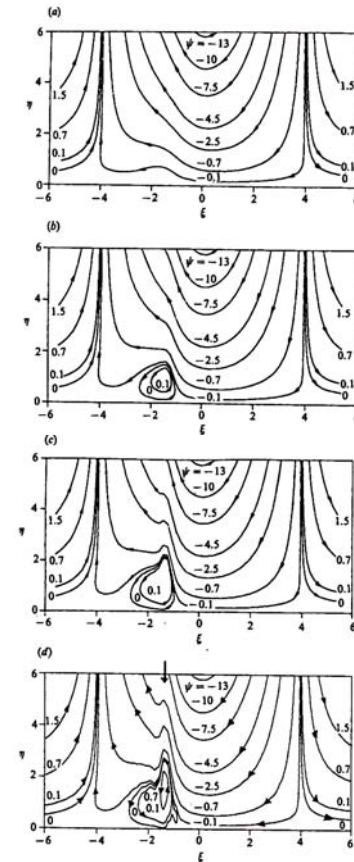
Algorithms that mimic the Ground Effect
Robins, Delisi, & Greene (2001)

- Robins, Delisi, & Greene (2001) devised a ground-effect algorithm which is also used in the current Eddy-Dissipation model (Sarpkaya, 2000; Sarpkaya, et. al., 2001). A summary of this algorithm is as follows:

- When the vortices approach an altitude of about $1.5b_0$ from the ground, a pair of inviscid image vortices are introduced and the decay rate is assumed to remain identical to that existing just above $1.5b_0$, (the assumed edge of the OGE).

- As the altitude of the vortices decreases further and reaches a level of $0.6b_0$, two secondary vortices (of relatively small strength) and their images are introduced, bringing the total number of real and image vortices to eight. Finally, when the satellite vortices have rotated 180 degrees around the primary vortices, a second set of ground-effect vortices (and their images) is introduced.
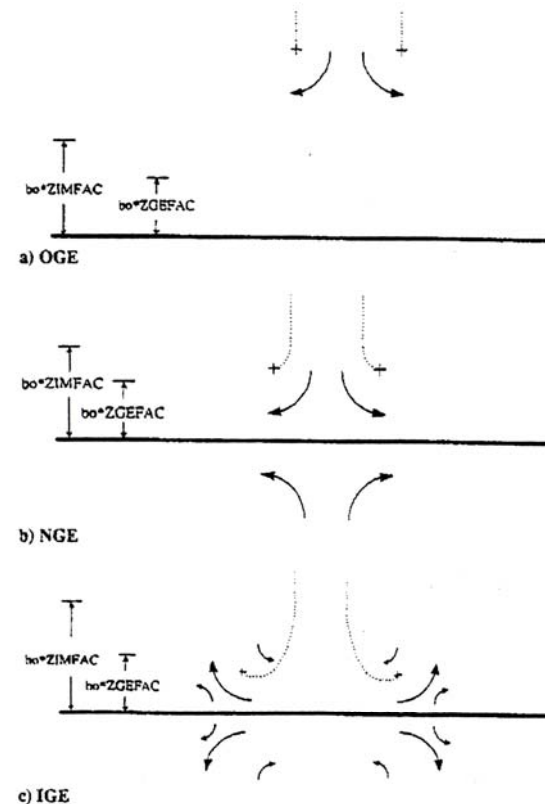

bo*ZIMFAC   bo*ZGEFAC

a) OGE

bo*ZIMFAC
bo*ZGEFAC

b) NGE

bo*ZIMFAC
bo*ZGEFAC

c) IGE

Fig. 1   Vortex geometry for algorithm phases.

Algorithms that mimic the Ground Effect
(Continued)

• This brings the total number of vortices to twelve. As in the image vortex region, the primary vortices (and their images) continue to decay in the ground-effect region at the rate that occurred just before the vortices entered the image vortex region.

• "The main benefit of the ground-effect vortices is that they enable, in a mechanical way, the observed simulation of the rebound of the primary vortices" (authors).

• The results depend on the judicious selection of the strengths and positions of the secondary and tertiary vortices and on the decay rates assigned to them. It mimics the observations but it is not a physics-based model.

• However, it must be noted that the various parameters (e.g., vortex locations and strengths) are determined from extensive comparisons with observations and results from LES.

• The effect of turbulence and separation enters into the calculations indirectly through the decay assigned to the vortices. Higher the turbulence, the smaller is the strength and rebound of the secondary vortices.

Algorithms that mimic the Ground Effect
(Continued)

- Typical results are shown in the accompanying figure together with MEM-1254 data (B-727/100).

- (Fig. a-left) shows altitude above the lidar van vs time after the passage of aircraft. The <u>asymmetry in the behavior of vortices</u> for t > 100 s is thought to be <u>due to the wind shear</u>. The algorithm does not include such effects.

- [Fig.(a), right] shows altitude vs lateral position and the effect of the wind.

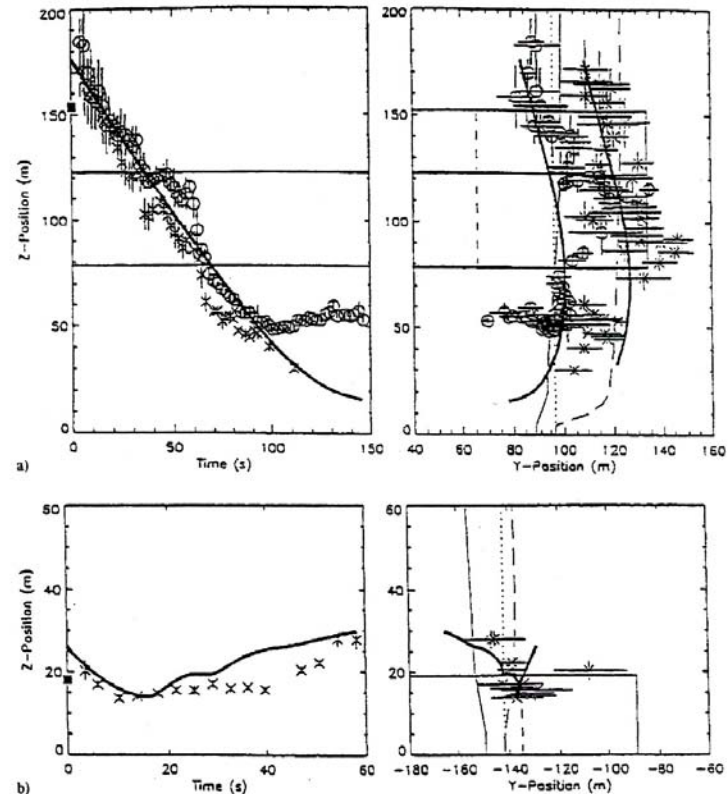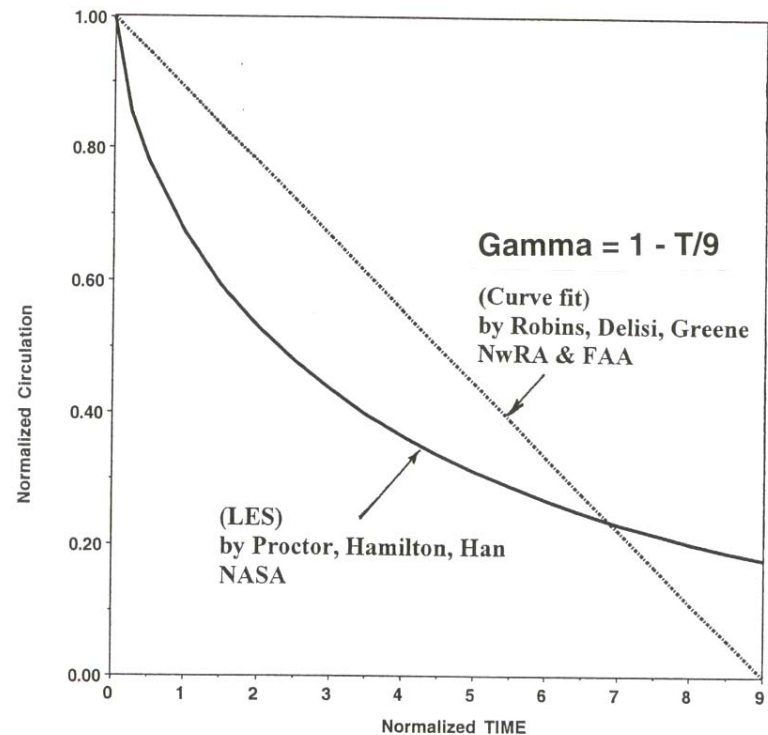- Fig. (2b) shows similar plots for a shorter time for MEM-1480, (only the starboard vortex is observed).

Fig. 2 Comparison of algorithm predictions and measurements for a) MEM case 1254 and b) MEM case 1480.

37

# Algorithms that mimic the Ground Effect
(Continued)

- The preliminary conclusions of Robins, Delisi, & Greene (2001) are:

- Vortices not interacting with the ground (OGE & NGE) decay faster in high turbulence, but are insensitive to turbulence after 20-30 s of their evolution;

- For OGE cases, the effect of high Turbulence is to increase the circulation decay rate by a factor of two;

- NGE results suggest that circulation decay of vortices IGE is independent of the ambient turbulence intensity.

- Figure compares their empirical model with the LES predictions of Proctor et al. (2000), (to be discussed in more detail later).

Gamma = 1 - T/9

(Curve fit)
by Robins, Delisi, Greene
NwRA & FAA

(LES)
by Proctor, Hamilton, Han
NASA

Normalized Circulation

Normalized TIME

38

"VORTEX" Model
Baren, Frech, Moet (2002)

• The "Vortex" is based on a simplified modeling approach of Greene (1986) and a simplified version of the IGE model of Robins, Delisi & Greene (2001). The differences are in the number and positions of the vortices introduced near the ground and the decay prescribed. Otherwise, the 'VORTEX' is an effort to mimic the events to match the measurements/observations rather than to develop a physics based Model. All major parameters (Boundary layer, turbulence intensification, flow separation, vortex shedding, etc.) do not directly enter into the 'Vortex'. Thus, it is a valiant effort to mimic MEM data through the use of a few line vortices at judiciously chosen positions.

rear view
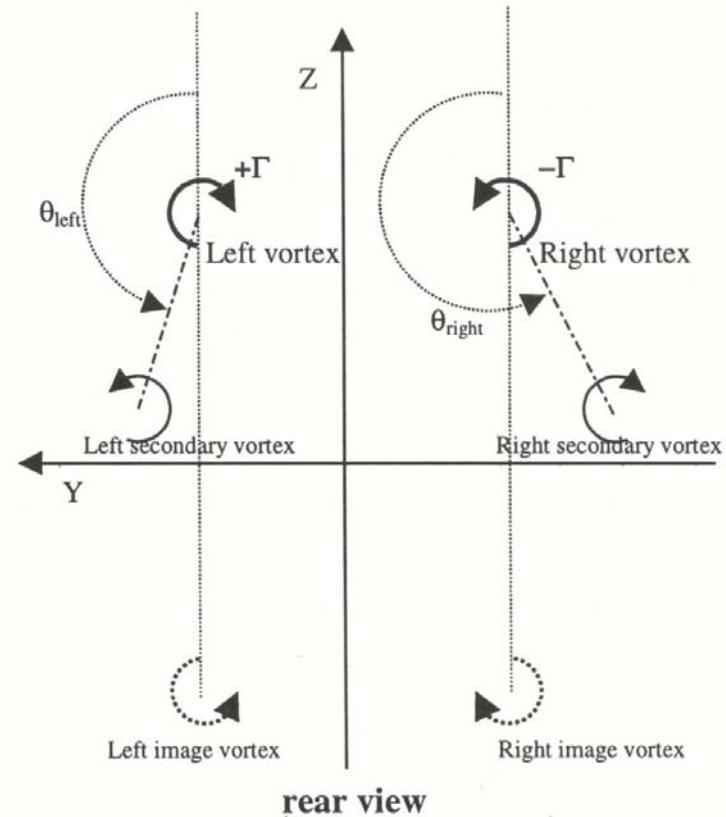
On Numerical Simulations

- As most aptly noted by Fischer and Patera (1994): "Fluid dynamics is, of course, not simply the solution of the Navier-Stokes equations for a particular configuration."

- "In many cases, the typically rather large parameter space precludes a purely numerical solution; analytical, heuristic, and experimental data, as well as intuition, must be brought to bear if the final goals are to be achieved."

- The numerical simulations are to be guided and inspired by ground-breaking measurements and flow visualization, mostly with non-intrusive techniques: Lidar and other means which will surely emerge in the years to come.

- These must be augmented with large-scale benchmark experiments to guide the numerical simulations at very large Reynolds numbers (with turbulence).

- DNS does not require 'modeling.' It deals only and purely with the numerical problem of solving the time-dependent N.-S. Eqs., albeit at relatively small Reynolds numbers.

Numerical Simulations

(Continued)

- Other computational methods include practically everything from mixing length to Reynolds stress models, advanced linear and non-linear eddy viscosity models, transient RANS models, and hybrid RANS/LES models.

- Efforts made to solve the N.-S. Eqs. at "high" **Re** by using a CONSTANT viscosity (smaller than that of the fluid) do not simulate the behavior of our nature. The results represent neither stable unsteady laminar flows nor unsteady turbulent flows!

- The position of the unsteady separation points and the very rapid increase of the intensity of turbulence towards them (van Oudheusden, 1999) must be accounted for. Simplistic models such as the approximate method of Kármán & Pohlhausen (1921) (based on a suitable velocity profile) cannot be used!

41

Numerical Simulations with LES

(Continued)

- At first sight, Large Eddy Simulation (LES) offered a bright new prospect for the computation of turbulent flows.

- By simulating the large scales of turbulent motion explicitly, the need for modeling is confined to the small scales which remain unresolved on the computational grid and are filtered away.

- Since the behavior of the small scales is universal, then the modeling task is straightforward and the errors induced by modeling are minimized.

- In a way, it appeared that all at once, the complexity, unreliability and controversy of traditional RANS turbulence modeling is rendered obsolete. Except that life and nature are not that simple!

- As Grinstein and Karniadakis (2002) noted recently: "After more than 30 years of intense research on large-eddy simulations (LES) of turbulent flows based on eddy-viscosity subfilter models, (Deardroff, 1970), there is now consensus that such an approach is subject to fundamental limitations.

42

Numerical Simulations with LES
(Continued)

- It has been demonstrated for a number of different flows that the shear stress and strain tensors involved in subfilter eddy-viscosity models have different topological features rendering scalar eddy-viscosity models inaccurate."

- Notwithstanding the concerns expressed by Grinstein and Karniadakis (2002), LES has been used by a number of investigators.

- Recently, Michelassi et al. (2003) expressed a more optimistic point of view in connection with their work on flow around low-pressure turbine blades at Reynolds numbers 5.18×10^4 and 2×10^5:

- "Direct numerical simulation and large-eddy simulation are able to provide a much deeper insight in the wake-boundary-layer interaction mechanism as compared to two-dimensional unsteady Reynolds averaged Navier-Stokes simulations."

- However, the independent use of LES at two different institutions on identical flows does not necessarily lead to identical results. Nevertheless, LES is the next best hope for the wake-vortex phenomena for (OGE, NGE, & IGE) simulations to provide creative guidance for the development of physics-based parametric models for the prediction of (operational) real-time response.

3-D LES of the sensitivity of vortex decay and transport in Ground Effect

Proctor-Hamilton-Han (2000)

• Proctor-Hamilton-Han (2000) have found that:

(a) Decay rates are strongly enhanced following maximum descent into GE;

(b) Normalized decay rate is insensitive to the initial values of circulation, height, and vortex separation;

(c) The simulations led to the decay rate:

$$\Gamma / \Gamma_{oo} = Exp\left[-\frac{2}{5}(T - T_{oo})^{2/3}\right]$$

where
• Γ: 5-15 m average circulation
• $T_{oo} = T_G + 0.25$
• $T_G : T \ at \ z = z_{min}$
• z_{min} : the minimum altitude achieved during vortex descent.

• The above decay-rate expression can only be applied for $T > T_{oo..}$

• It is shown (for the cases computed) that the proposed decay rate is independent of the ambient turbulence. This may be due to the fact that the strong deceleration of the vortex-induced BL doubles the intensity of the wall turbulence, obscuring the effect of the prevailing ambient turbulence .

Vortex Decay Rate

The figure on the right shows that $d\Gamma/dt = -1/9 \cong -0.11$ (Robins, et al., 2001).
The figure on the left shows that $d\Gamma/dt$ is highly nonlinear (Proctor et al., 2000).
This points out the important fact that it may be misleading to draw mean lines or
upper or lower bounds through the Wake Vortex data, particularly IGE region.
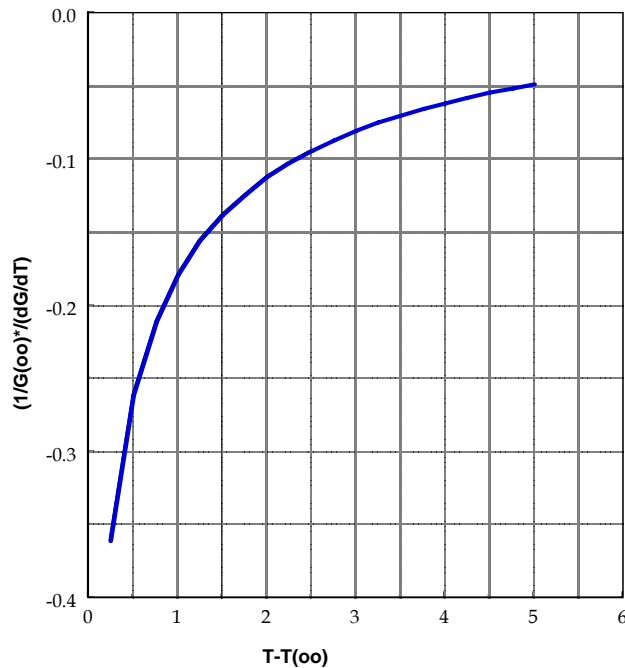
Rate of change of circulation with time

Gamma = 1 - T/9

(Curve fit)
by Robins, Delisi, Greene
NwRA & FAA

(LES)
by Proctor, Hamilton, Han
NASA
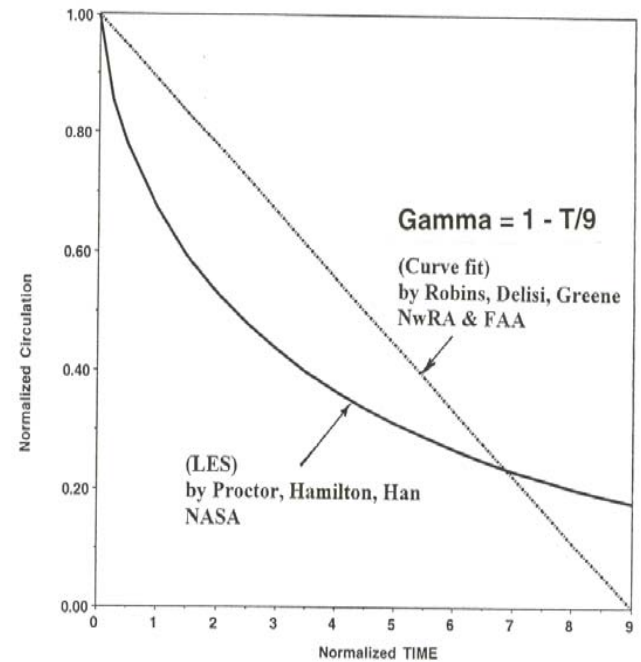
• Five experiments were conducted for a vortex initialization height. Comparisons of the experiments are shown in figure as a function of the normalized time. The time coordinate for each experiment is offset by $T_G = T(z_{min})$.

• The normalized 5-15 m average circulation and lateral positions tend to collapse when T_G is accounted for.

• Vortex decay is significantly increased after maximum penetration into IGE zone.

• The enhanced decay begins at about (0.25x normalized time) following T_G. It is independent of the ambient turbulence, (to be discussed shortly).
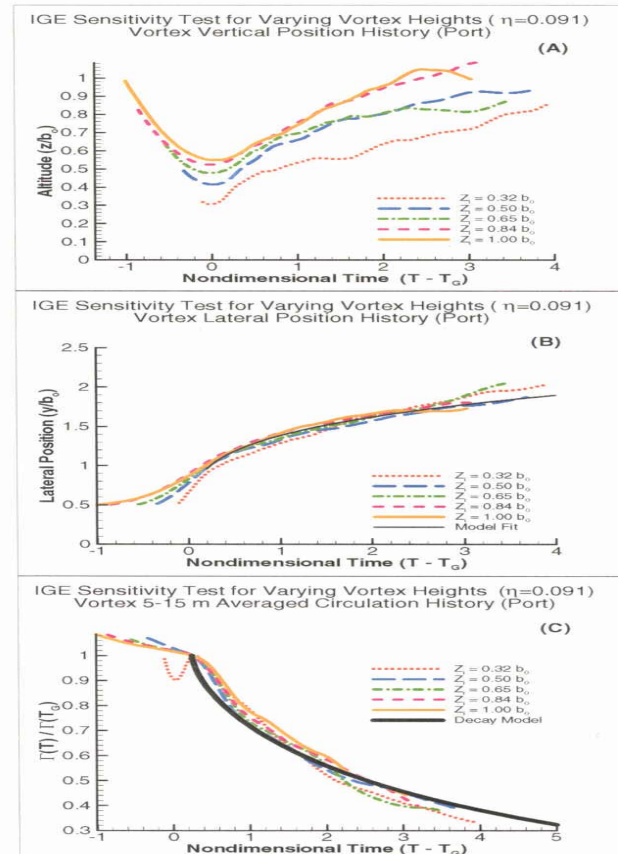
Figure 2. *Sensitivity to vortex initiation height. Nondimensional height (a), nondimensional lateral position (b), and nondimensional 5-15 m average circulation (c) vs nondimensional time. "Decay model" in (C) from Eq.1 and "Curve fit" in (B) from Eq.2.*

46

3-D large-eddy Simulation
Proctor-Hamilton-Han (2000)
(Continued)

- **Sensitivity to initial separation:**

  Figures on the left show the IGE sensitivity for varying separation (b_o) for vortex altitude, lateral position (including model fit), and average circulation (including decay model).

- **Sensitivity to initial circulation:**

  Figures on the right show the IGE sensitivity for varying initial circulation for vortex altitude, lateral position (including model fit), and average circulation (including decay model).

- Clearly, the proposed formulas for IGE decay and lateral drift are in excellent agreement with the LES predictions.
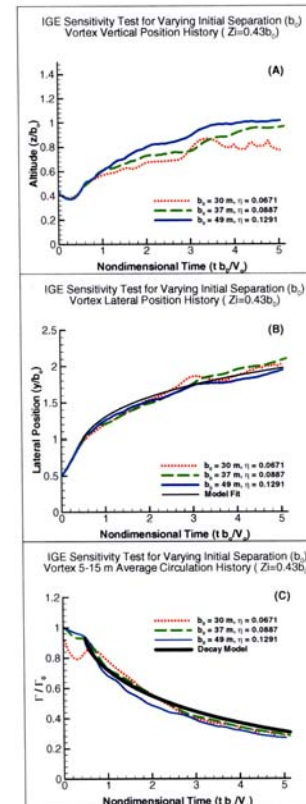
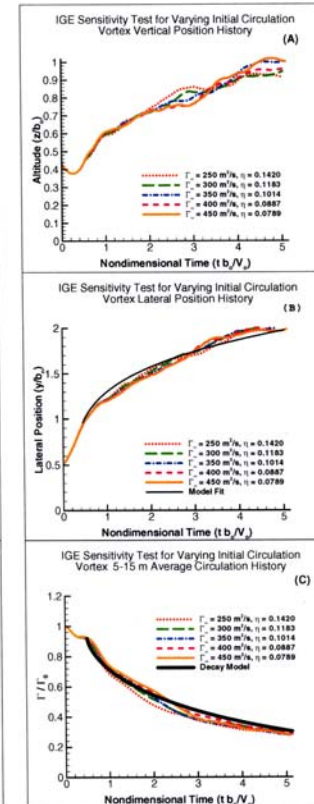Figure 3. Same as Fig. 2, but for sensitivity to initial vortex spacing.

Figure 4. Same as Fig.2, but for sensitivity to initial vortex circulation.
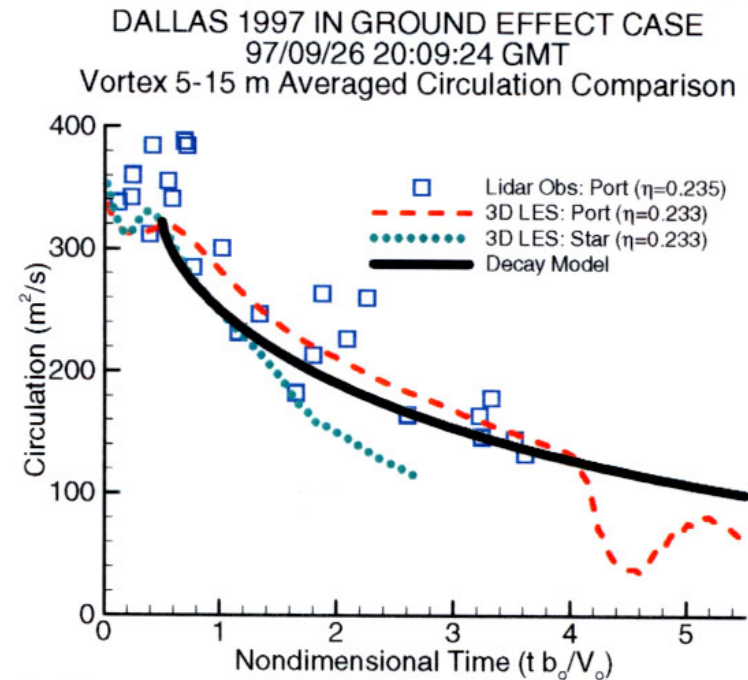
3-D large-eddy Simulation
Proctor-Hamilton-Han (2000)
(Continued)

• A comparison of the IGE decay model with the LES simulation of the landing of an aircraft (L-1011).

• The authors noted that "The slightly faster decay of the starboard vortex may be due to the opposite sign vorticity of the ambient crosswind" (the initial profiles of ambient potential temperature and cross wind are given in the paper).

In summary, the results show that:

• Vortex decay for IGE has minor sensitivity to ambient turbulence. This is in conformity with other supporting evidence noted earlier.

• Both the decay and drift models show very good agreement with the LES results and could be used to build a MODEL with confidence with further simulations.

• Ground linking shows sensitivity to relatively high levels of the ambient turbulence (next slide). The effect of the crosswind shear on the sensitivity of all the parameters noted above remains unresolved.

DALLAS 1997 IN GROUND EFFECT CASE
97/09/26 20:09:24 GMT
Vortex 5-15 m Averaged Circulation Comparison

Legend:
□ Lidar Obs: Port (η=0.235)
— — — 3D LES: Port (η=0.233)
• • • • • 3D LES: Star (η=0.233)
—— Decay Model

X-axis: Nondimensional Time ($t\, b_o/V_o$)
Y-axis: Circulation (m^2/s)

3-D large-eddy Simulation
Proctor-Hamilton-Han (2000)

η (nondimensional eddy dissipation rate) = 0.2333 (left): (NO GROUND LINKING)
η = 0.3886 (right): (WITH GROUND LINKING).
NO GROUND LINKING (for η < 0.3)

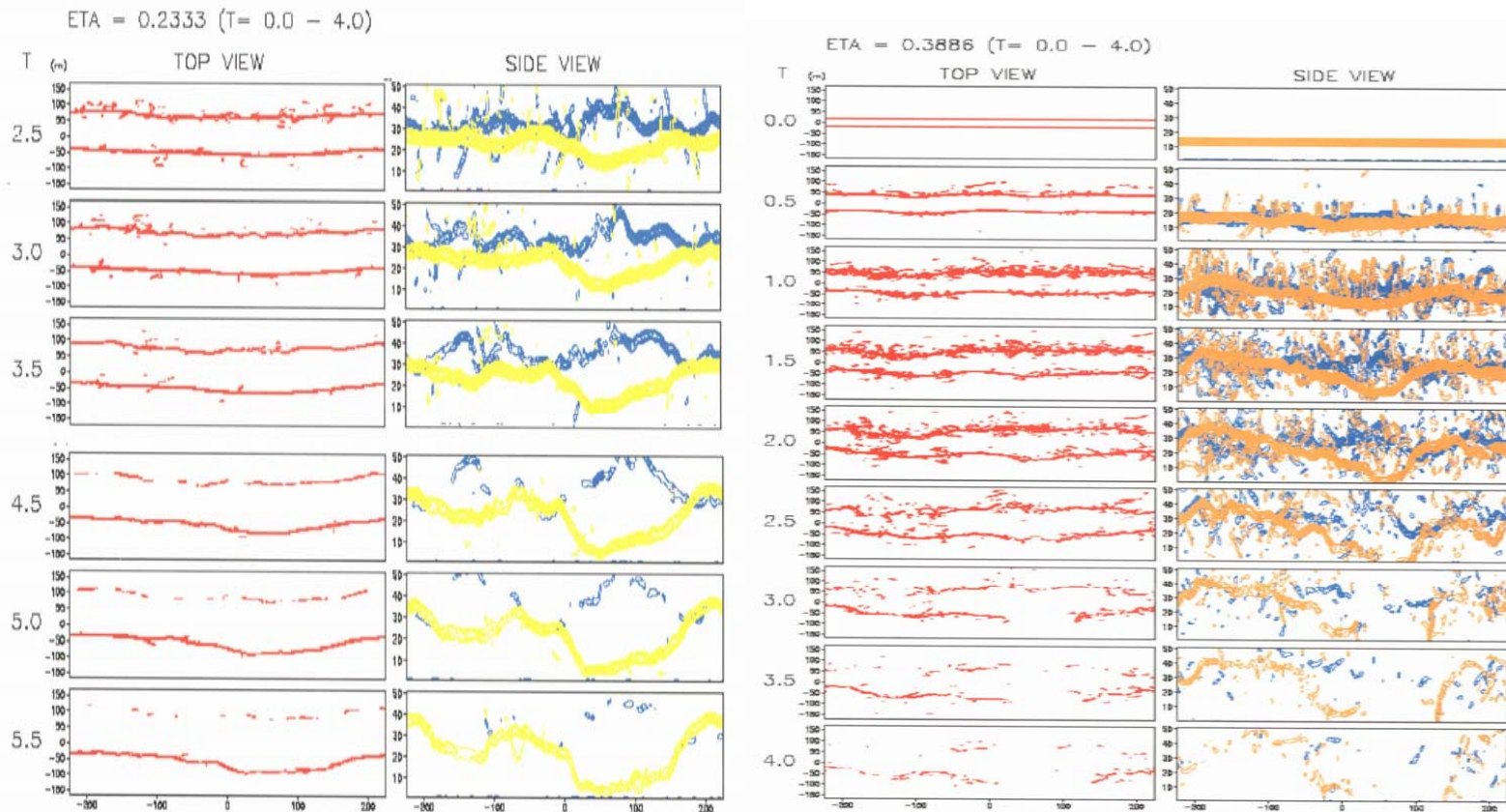**Figure 8.** *Same as Fig. 7, but for η = 0.233.*

igure 7. *Time evolution within IGE of wake vortex pair for η = 0.388. Top (x,y) and side (x,z) view of wake vortices at increments 0.5 nondimensional time units.*

Probabilistic Two-Phase Wake Vortex Decay and Transport Model (**P2P**)
(Jour. Aircraft, 40, 323-331, 2003)
F. Holzäpfel

- P2P is designed to predict the bounds of wake vortex behavior in a probabilistic sense.

- The evolution of the normalized circulation $\Gamma(r,t)/\Gamma_o = \Gamma^*_{(5-15)}$ is described by two consecutive decay phases: the <u>diffusion</u> phase and the <u>rapid decay</u> phase.

- The parameters of the two phases are determined from the available data and as functions of the meteorological parameters.

- Figure shows circulation from LES and respective fits of P2P for various degrees of turbulence and stratification.

- P2P accounts for all relevant parameters (wind turbulence, stable stratification, and ground proximity, <u>with the exception of shear</u>, after the numerical simulations are transferred to the real-time model by the adjustment of the parameters.
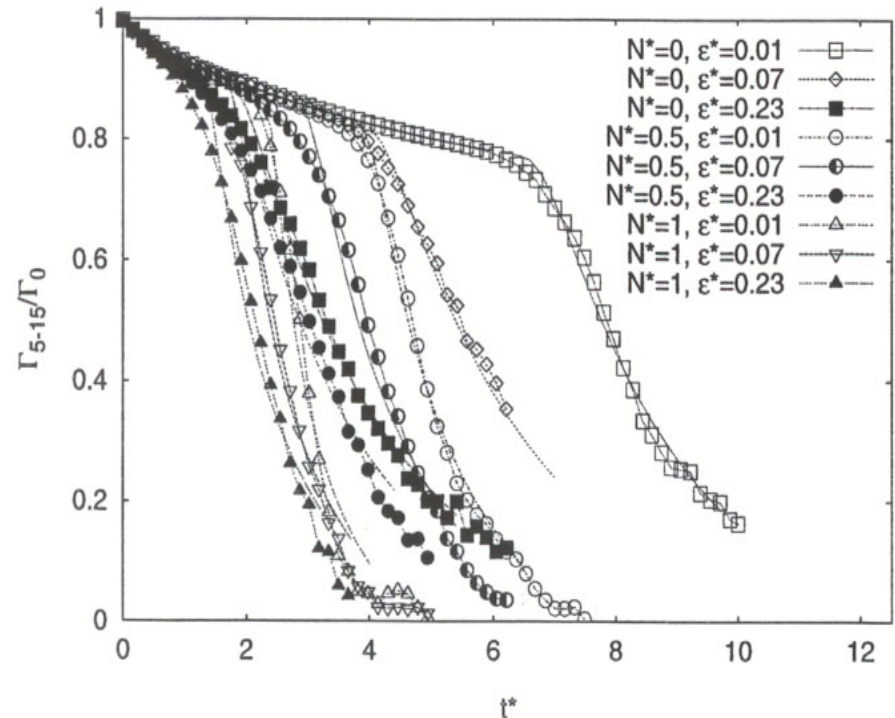
Assessment of P2P

Holzäpfel & Robins (2004)

A preliminary assessment of the P2P by Holzäpfel & Robins concluded that:

- "The uncertainty allowances appear appropriate."
- "The comparison of a deterministic version of P2P to Sarpkaya's model [Ref. 5] yields good results."
- "The spatio-temporal wind variability is significant."
- "In the majority of the cases, the probabilistic predictions of P2P are conservative."
- "Only flawed crosswind information or pronounced wind shear can cause deficient predictions."
- "Constant wind shear can prolong vortex lifetime, whereas shear layers can modify vertical and lateral transport."
- "Vortex decay proceeds too slowly for appreciable capacity benefits, whereas lateral vortex drift bears considerable potential for safe reduced spacing operations."
- "A future goal would be to improve short-term weather forecasts by the assimilation of local weather observations."

Vortex Element Method
(**A Method of thousand Schemes!**)

- Once upon a time Vortex Element Method (VEM) was a matter of some interest to the fluid dynamics community. It looked like as though there might be some opportunity for research, and a few people in 1970's (Gerard, Sarpkaya, Maull, Kuwahara) were predicting the kinematics and dynamics of flow about cylinders and flat plates.

- The shortcomings of the model were forgiven at its infantile stages. However, it became quickly clear that there is no Reynolds number, diffusion is arbitrary, and the model calls for large numbers of ad hoc schemes and for more CPU.

- In the meantime, computer power increased enormously, DNS (at relatively low Re), RANS & FANS at higher Re, LES (for high-Reynolds-Number incompressible as well as compressible turbulent wall-bounded flows), the coupling of LES with RANS, and the interfacing of statistical turbulence closures with LES became possible.

- In view of this enormous progress, the funds and applications for VEM dried up.
    It became clear that VEM had been initially over hyped.

Vortex Element Method
(Continued)

- Currently, VEM is not an area of active research or application as most aptly noted by PG Saffman & DW Moor. In a recent NASA (Larc) report, Gainer (2002) noted that "The problem with discrete-vortex methods is that they are inherently inaccurate." Our extensive review "Sarpkaya, T., (1994), *Vortex Element Methods for Flow Simulation*, In Advances in Applied Mechanics, *(Ed. Th. Wu and A Hutchinson),* Vol. 31, pp. 113-247, Academic Press, London" London" clearly pointed out its severe limitations.

- In short, isolated line vortices, vorticity blobs, vortex balls or vortons, or toroidal vortices are introduced into an inviscid flow field and tracked numerically either by a Lagrangian or mixed Lagrangian-Eulerian scheme. This is, however, easier said than done: The most important difficulty is that while a viscous vortex can be created, convected, diffused, and decayed (through the cancellation of oppositely-signed vorticity), an inviscid vortex can neither be diffused nor decayed.

- Often, each vortex element is assumed to be a Lamb vortex. It involves a Gaussian vorticity distribution and a circumferential velocity given by,

$$\omega(r,t) = (\kappa_o/2\pi\nu t) \exp(-r^2/4\nu t)$$

and

$$v(r,t) = (\kappa_o /r) [1 - \exp(-r^2/ 4\nu t)]$$

Vortex Element Method
(Continued)

• Obviously, *not even a single vortex with a compact support* (e.g., a Rankine vortex with an invariant *finite core* or *compact cross section* in which all of the vorticity is concentrated) is an exact solution of the Navier-Stokes equations.

•A single Lamb vortex (which has an infinite support in an unbounded domain) is an exact solution. However, the velocity field of a <u>multi-Lamb-vortex system</u> is not an exact solution because the nonlinearity of the Navier-Stokes equations does not permit the superposition, without deformation, of a finite number of vortex fields.

• An *inviscid vortex* can only be created and convected. The artificial spreading of its core and the reduction of its strength through various schemes (contrary to Helmholtz's laws,1858) only lead to non-quantifiable errors.

• Its users resorted to retrofitting the model predictions to the existing data through the use of a large number of schemes using artificially defined Reynolds numbers and assumptions which defy the laws of dynamics.

• Reynolds number is changed by changing the <u>kinematic viscosity</u> and then it is given new names like "eddy viscosity" or "turbulence viscosity", implying that the results are for a turbulent flow and the calculations dealt with turbulence. The fact of the matter is that the solution is still for a laminar flow (if it were correct in all other aspects!) But then, why use DVM for a laminar flow when there are so many other excellent N.S. codes (including RANS, FANS, DNS, just to name a few).

VEM
(continued)

- If, on the other hand, the diffusion process is to be considered turbulent, then the choice of the turbulent diffusion coefficient and the turbulent length scale distribution are unknown parameters.
  This brings one back to square one!
  Turbulence modeling.

- It has also clear that the random-walk method, like the Vortex-in-Cell (VIC) method, does not and cannot prescribe a specific Reynolds number. In fact, the Reynolds number mimicked in all vortex models is that of the experiments and/or finite-difference calculations to which the numerical predictions are retrofitted or with which the numerical schemes are calibrated.

- Figure shows the use of constant-core Lamb vortices which need to be heavily overlapped to somewhat smoothen the velocities calculated.
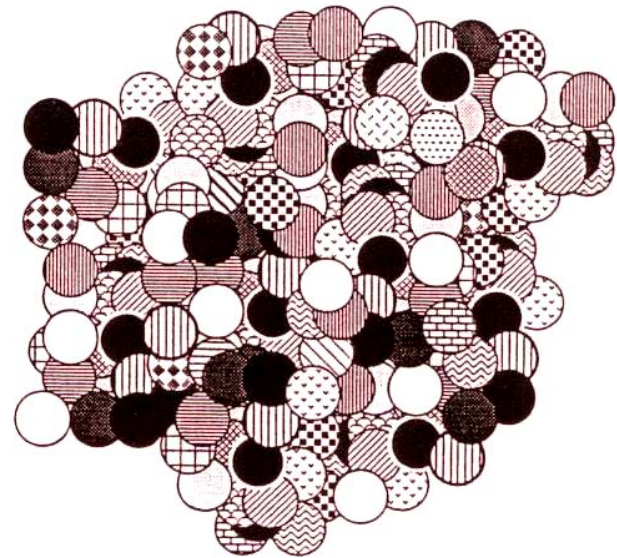
VEM
(continued)

- The equations of motion and force were first given by Sarpkaya in 1963 for a flow about a circular cylinder. Since than it has been "re-derived" in many Ph.D. thesis!

- Sarpkaya, T., 1963, "Lift, Drag, and Added-Mass Coefficients for a Circular Cylinder Immersed in a Time-Dependent Flow," *J. Appl. Mech., ASME*, Vol. 85, Ser. E., pp. 13-15.

- This was followed by two more papers:

- Sarpkaya, T., 1969, "Analytical Study of Separated Flow About Circular Cylinders," *Phys. of Fluids*, Vol. 12, Supplement II, p. 145.

- Sarpkaya, T., 1975, "An Inviscid Model of Two-Dimensional Vortex Shedding for Transient and Asymptotically Steady Separated Flow over an Inclined Flat Plate," *J. Fluid Mech.*, Vol. 68, pp. 109-128.

- Sarpkaya, T., and Shoaff, R. L., 1979, "An Inviscid Model of Two-Dimensional Vortex Shedding for Transient and Asymptotically Steady Separated Flow Over a Cylinder," *AIAA J.*, Vol. 17, No. 11, pp.

VEM
(continued)

- and culminated in two major review papers:

- Sarpkaya, T., (1989), "Computational Methods with Vortices–The 1988 Freeman Scholar Lecture," *Journal of Fluids Engineering*, ASME lll, No. 1, pp. 5-52.

- Sarpkaya, T., (1994), *Vortex Element Methods for Flow Simulation*, In <u>Advances in Applied Mechanics</u>, (*Ed. Th. Wu and A Hutchinson),* Vol. 31, pp. 113-247, Academic Press, London.

- In 1973 Chorin proposed to solve the 2-D Navier-Stokes Eqs. using discrete vortices subjected to random walk:

- Chorin, A. J., (l973), "Numerical Study of Slightly Viscous Flow," *J. Fluid Mech.*, Vol. 57, pp. 785-796.

- Chorin, A. J., and Bernard, P. S., (l973), "Discretization of a Vortex Sheet with an Example of Roll-up," *J. Comput. Phys.*, Vol. 13, pp. 423-429.

- Chorin, A. J., (l978), "Vortex Sheet Approximation of Boundary Layers," *J. Comput. Phys.*, Vol. 27, pp. 428-442.

VEM
(continued)

- It appeared at first that VEM will be an exciting method in fluid dynamics. However, it soon became clear that <u>chaos awaits at the end of the road</u>. One has to devise large number of schemes to keep it going.

- In short it ceased to be a method. Workers of VEM moved on to RANS, DNS, LES, etc.

- There are very few cases where its simplified version with **fewer vortices** may be used to predict **inviscid flow behavior** in flows where the viscous effects are not important (e.g., opening of a parachute). Otherwise, powerful computers, reliable finite-difference codes, spectral methods have buried the DVM. The IGE problem is dominated by viscosity, turbulence, stratification, wind/shear, instabilities, unsteadiness, and strong pressure gradients IGE and thus not a good candidate for VEM.

- Winckelmans & Ploumhans (1999) noted that "The Method of Discrete Vortices (MDV) appears as the most suitable method for the problem of efficient wake simulations within the context of Computational Fluid Dynamics (CFD)." They have further noted that "Indeed, this method has the potential to lead to a CFD-based real-time Vortex Forecast System (VFS) in a truly operational airport environment." Their enthusiasm is not supported by the facts of the past 30 years and by their application of VEM (they called it DVM) to the ground effect with constant viscosity!

VEM

- The figure shows the roll-up of a vortex sheet and the development of chaos near the core.

- Numerous schemes have been devised to maintain the sheet smooth but the results were always the same:

chaos awaits at the end of the road.
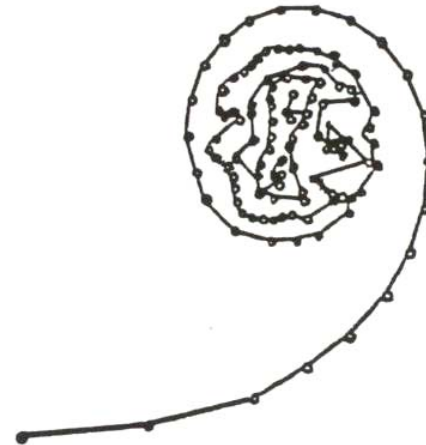
VEM (continued)

• As noted earlier, VEM can be used when the effects of viscosity is negligibly small and the duration of motion is relatively short. This helps to minimize the consequences of diffusion and decay as in the case of an impulsively-started flow about a parachute canopy.

• One can approximately calculate the pressure forces, added mass, and the flow kinematics.

(from: Sarpkaya, T., (1991), *"Methods of Analysis for Flow Around Parachute Canopies,"* Proceedings of the 11th AIAA Aerodynamic Decelerator Systems Technology Conference, AIAA-91-0825, pp. 1-17.)
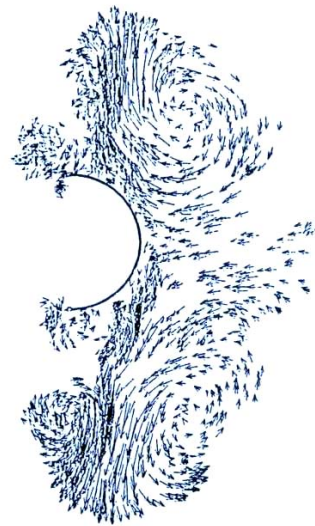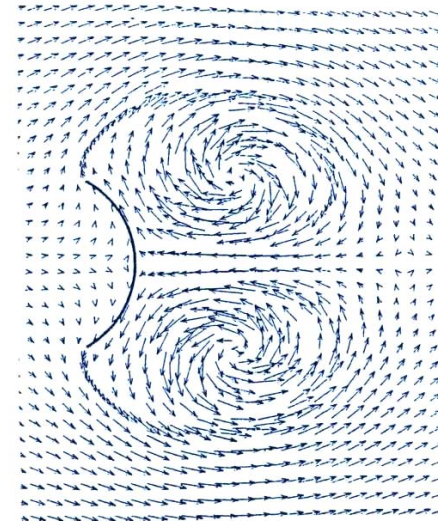
(a)   (b)

VEM (continued)

• Figure by Winckelman & Ploumhans (1999) shows at t =60 (no wind) the vortex positions for three different values of "constant and uniform viscosity." " Vorticity diffusion is done by spreading the core associated with each particle" which "degrades" and "eventually becomes very large," as noted by the authors.

• There are too many schemes in their calculations. For example, they speak of "variable effective viscosity"and then state that "it has to come either from additional validated modeling or from additional experimental data."

Then they use a constant and uniform viscosity. This could only produce a LAMINAR flow if and only if everything else were precise, as in N.-S. solutions of Zheng and Ash (1996).

Influence of effective viscosity (no wind, t=60s)

• $v^* = 0.125 \ m^2 s^{-1}$
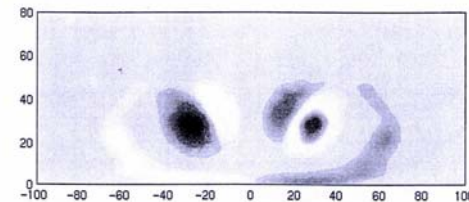
• $v^* = 0.25 \ m^2 s^{-1}$
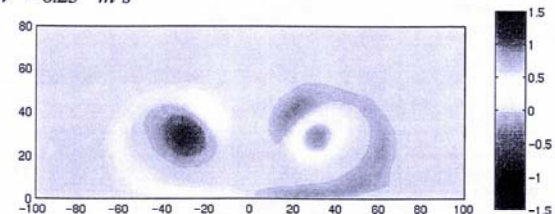
• $v^* = 0.5 \ m^2 s^{-1}$

61
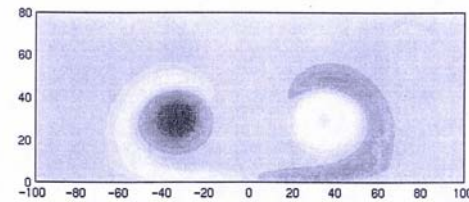
VEM (continued)

- They have developed two methods (A & B).

- Method A "does not lead to a method that satisfies zero-slip condition" on the runway, as noted by the authors.

- Method B is made to satisfy the zero-slip condition by introducing a vortex sheet of necessary circulation per unit length to cancel the slip velocity. All using a <u>constant viscosity</u> as in laminar flow!

- Separation points are calculated by SABIGO using Integral-Momentum equation (with too many unwarranted assumptions). This will be taken up shortly.

- The Method B is too CPU demanding to be an operational model, as noted by the authors.

Influence of wind
$v^* = 0.25 \ m^2 s^{-1}, \qquad t = 30 \ s$

- $U_w = 0.5 \ m s^{-1}$

- $U_w = 1.0 \ m s^{-1}$

- $U_w = 2.0 \ m s^{-1}$
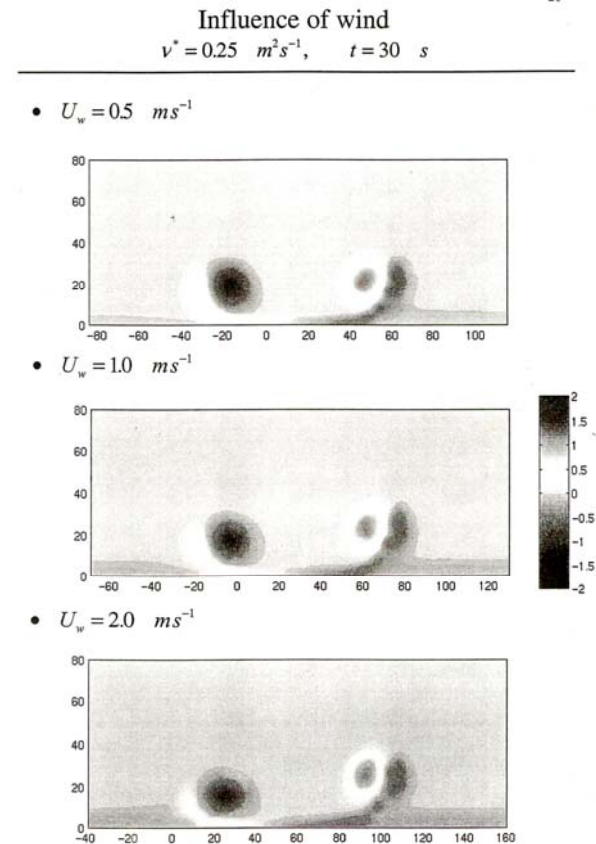
VEM (continued)

- Comparison of the results of the two methods:

- Top: Method B (with no slip), and

- Bottom: Method A (with slip on the ground).

- All with a constant and uniform viscosity!

Comparison of two methods

$$U_w = 0 \quad ms^{-1}, \qquad v^* = 0.25 \quad m^2 s^{-1}, \qquad t = 90 \quad s$$

no-slip

slip
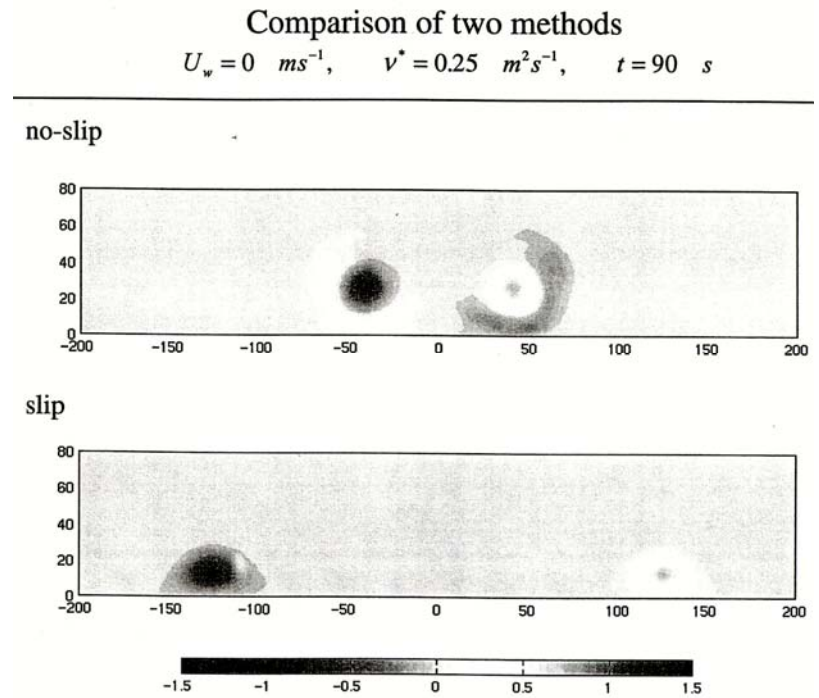
Belotserkovsky & his company, SABIGO, Ltd.

- Belotserkovsky (1999, TP13373E, Sabigo; "*Computer Vortex Forecast System*", VFS), in cooperation with G. S. Winckelmans attempted to apply the integral-momentum equation to Ground Effect.

- His formulations are very obscure and certainly far from those given in texts like (Schlichting & Loitsyanskiy). His analysis needs eight experimental parameters. There is no explanation as to how the decelerating boundary layer flow was represented. Belotserkovsky gave only two references: (*Jane's All the World's Aircraft*, 1997-1998), and (*The Complete Encyclopedia of World Aircraft,* 1997).

- The figure on the right is the velocity due to the primary vortices!

- His report has not been subjected to the scrutiny of a journal review and does not contain sufficient information for consideration for IGE.
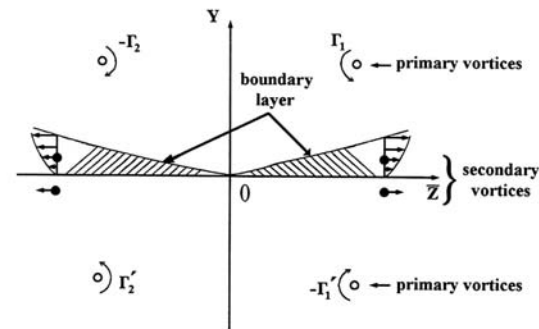
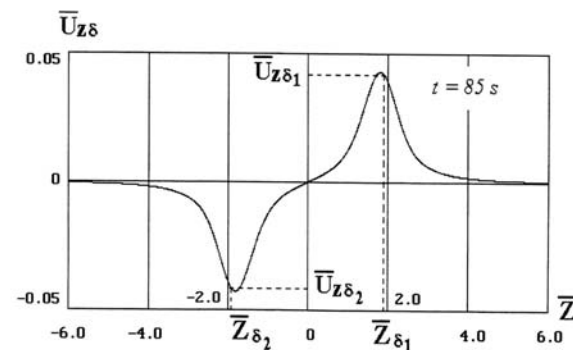Fig. 6.1. The calculation scheme for the ground boundary layer

Fig. 6.2. The vortex velocity (without the velocity generated by the secondary vortices) on the ground surface

64

13. Integral Methods for Calculation of Turbulent Boundary Layers

Among the semiempirical methods of turbulent boundary layer calculation that are discussed later, an important role is played by integral semiempirical methods based on the application of the Prandtl mixing length theory.

We shall pause on the basic techniques of integral methods, referring the reader for the details to a thoroughly composed monograph,[107] the first part of which is concerned with the detailed presentation of integral methods.

In its initial form the idea of the integral method was in the determination of velocity profiles in the sections of a turbulent boundary layer by assigning polynomial approximations of turbulent skin friction τ and the mixing length l in the formula

$$U - u = \int_y^\delta \sqrt{\frac{\tau}{\rho}} \frac{dy}{l} \tag{192}$$

approximations for the skin friction

$$\frac{\tau}{\tau_w} = \sum_{i=0}^{n} \alpha_i \eta^i \qquad \eta = \frac{y}{\delta} \tag{193}$$

where δ is the finite boundary layer thickness, or of the polynomial representation which is more convenient for calculations

$$\sqrt{\frac{\tau}{\tau_w}} = \sum_{i=0}^{n} b_i \eta^i \tag{194}$$

The coefficients a_i and b_i in these formulas are selected from the corresponding boundary conditions, the examples of which are

$$\frac{\tau}{\tau_w} = 1 \qquad \frac{d}{d\eta}\left(\frac{\tau}{\tau_w}\right) = \beta \qquad \frac{d^2}{d\eta^2}\left(\frac{\tau}{\tau_w}\right) = 0 \quad \text{at} \quad \eta = 0$$

$$\frac{\tau}{\tau_w} = 0 \qquad \frac{d}{d\eta}\left(\frac{\tau}{\tau_w}\right) = 0 \qquad\qquad\qquad \text{at} \quad \eta = 1 \tag{195}$$

13.1.6 Integral Relations and Integral Methods

Just as for steady boundary layers, integral equations can also be derived from the boundary–layer equations for unsteady boundary layers. For boundary layers with constant physical properties and neglecting the dissipation they read:

$$\frac{\partial}{\partial t}(U\delta_1) + \frac{\partial}{\partial x}(U^2\delta_2) + \delta_1 U \frac{\partial U}{\partial x} + jU^2 \frac{\delta_2}{r_w}\frac{dr_w}{dx} = \frac{\tau_w}{\varrho}, \tag{13.14}$$

$$U^2\frac{\partial\delta_1}{\partial t} + \frac{\partial}{\partial t}(U^2\delta_2) + \frac{\partial}{\partial x}(U^3\delta_3) + jU^3\frac{\delta_3}{r_w}\frac{dr_w}{dx} = \frac{2}{\varrho}\mathcal{D}, \tag{13.15}$$

$$U\frac{\partial U}{\partial t}\frac{\delta_T}{c_p} + \frac{\partial}{\partial x}[(T_w - T_\infty)U\delta_T] + j(T_w - T_\infty)U\frac{\delta_T}{r_w}\frac{dr_w}{dx} = \frac{q_w}{\varrho c_p} \tag{13.16}$$

with $j = 0$ for plane boundary layers, and $j = 1$ for axisymmetric boundary layers. For steady boundary layers, these equations become Eq. (12.10) to (12.12). An extension of the integral equations to compressible flows of the ideal gas has been given by H. Schlichting (1982), p. 414.

In analogy to the approximate methods for steady boundary layers described in Chap. 8, corresponding methods for unsteady boundary layers have also been developed. H. Schuh (1953), K.T. Yang (1959), L.A. Rozin (1960), M. Holt; W.-K. Chan (1975) and M. Matsushita et al. (1984a, 1984b) have all presented integral methods of this kind, and the method of K.T. Yang also treats the thermal boundary layer. Here the fundamental equations used are the integral relations (13.14) to (13.16). Either polynomials or profiles from similar solutions are used for the profiles of the velocity and the tempera-

The mixing length l is also presented by different approximate expressions from which we note the following:

1. According to Prandtl

$$l = \mathrm{æ}y \quad \text{and} \quad \frac{l}{\delta} = 0.14 - 0.08\left(1 - \frac{y}{\delta}\right)^2 - 0.06\left(1 - \frac{y}{\delta}\right)^4$$

2. According to Kutateladze and Leontiyev

$$\frac{l}{\delta} = \frac{\mathrm{æ}y}{\delta} - (2\mathrm{æ} - 3\gamma)\left(\frac{y}{\delta}\right)^2 + (\mathrm{æ} - 2\gamma)\left(\frac{y}{\delta}\right)^3 \qquad \mathrm{æ} = 0.39 \qquad \gamma = 0.14$$

3. According to the paper of the Stanford Conference (see the earlier reference)

$$\frac{l}{\delta} = \left(\frac{l_\delta}{l}\right)\mathrm{th}\left[\frac{\mathrm{æ}\,(y/\delta)}{l_\delta/l}\right] \qquad \mathrm{æ} = 0.41 \qquad \frac{l_\delta}{l} = 0.085$$

4. According to Chi and Chang

$$\frac{l}{\delta} = 0.4\frac{y}{\delta} - 0.5\left(\frac{y}{\delta}\right)^2 + 0.2\left(\frac{y}{\delta}\right)^3$$

5. According to Escudier and Spalding:

$$\frac{l}{\delta} = \frac{\mathrm{æ}y}{\delta} \quad \left[0 \leq \frac{y}{\delta} \leq \left(\frac{1}{\mathrm{æ}}\right)\frac{l_\delta}{\delta}\right] \qquad \frac{l}{\delta} = \frac{l_\delta}{\delta} \quad \left[\left(\frac{1}{\mathrm{æ}}\right)\left(\frac{l_\delta}{\delta}\right) \leq 1\right]$$

There is some arbitrariness in the selection of the profiles of τ and l for the boundary layer cross-sections, which is sometimes moderated by additional intuitive considerations.

factor $H = \delta_1 / \delta_2$, which is the ratio of the replacement thickness δ_1 and the impulse loss factor δ_2 for the boundary layer. The equations are:

$$\frac{dR_2}{dZ} = \tfrac{1}{2}\,\mathrm{Re}\,U_{z_\delta}C_f - \frac{U_{z_\delta}'}{U_{z_\delta}}(H+1)R_2 \tag{6.1}$$

where $R_2 = \dfrac{U_{z\delta}\delta_2}{\nu}$; ν is the viscosity coefficient; $\mathrm{Re} = \dfrac{U_{z\delta}l}{\nu}$; l is the wingspan; $U_{z\delta}$ is the vortex velocity component directed along Z-axis (Fig. 6.1) on the border of the boundary layer; $U_{z\delta} = \dfrac{U_{z\delta}}{U}$ (U is the aircraft flight speed); and $Z = \dfrac{Z}{l}$; $U_{z\delta}' = \dfrac{dU_{z\delta}}{dZ}$;

$$C_f = C_{f0}\left[1 + \lambda_1 f + \lambda_2\left(e^{\lambda_3 f} - 1\right)\right]; \tag{6.2}$$

$$H = H_0\left(1 - \lambda_4 f\right) - 0.019\,fe^f\,\xi. \tag{6.3}$$

Here the index 0 corresponds to the quantities at $Z = 0$. Eqs. (6.2), (6.3) contain the following experimental parameters:

$$\lambda_1 = 0.2814 - 0.036\xi + 36\xi^{-4.5}$$
$$\lambda_2 = 0.118\xi - 0.262$$
$$\lambda_3 = 0.585 - 0.125\xi + 20.4\xi^{-4.5}$$
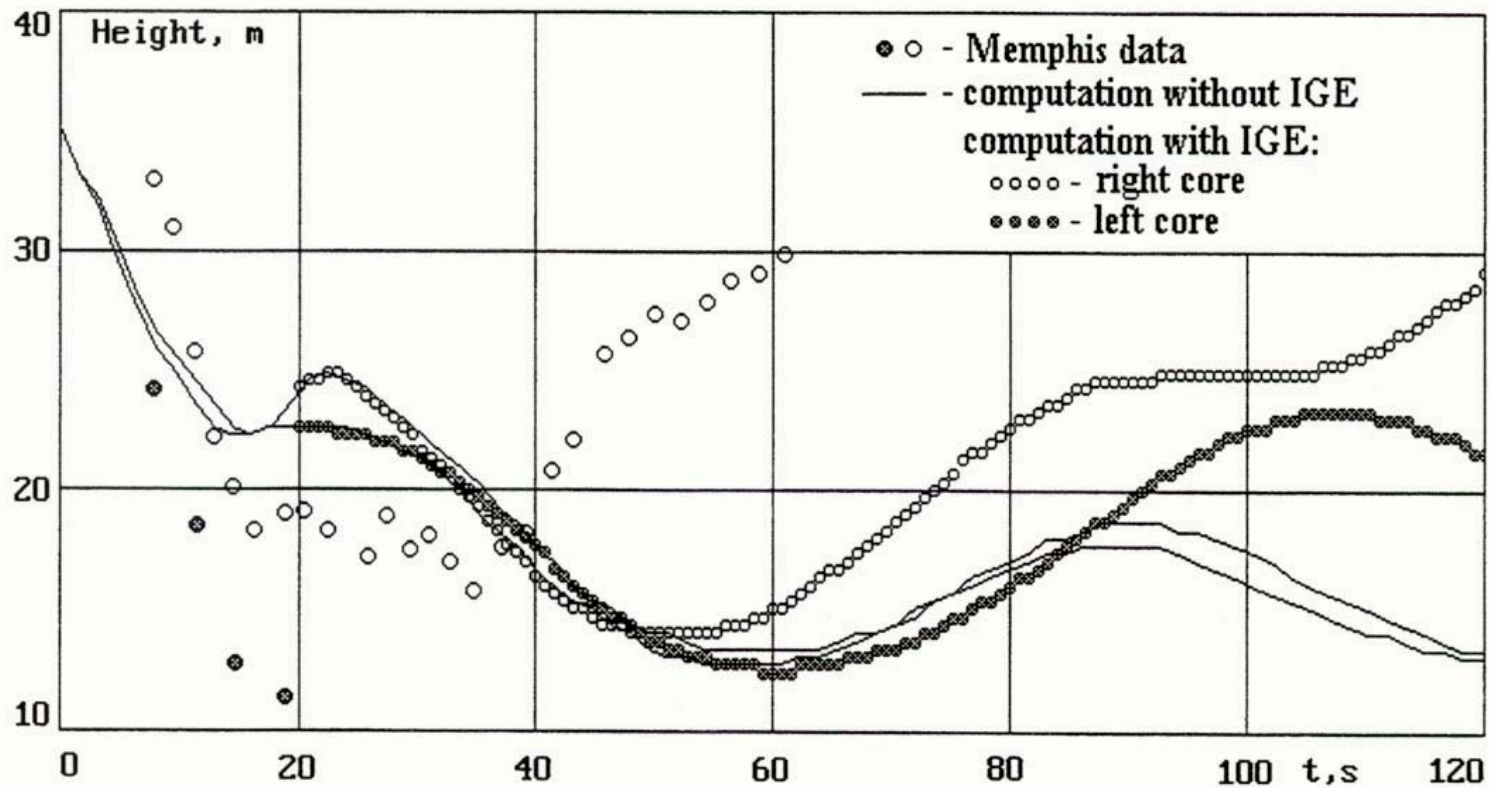$$\lambda_4 = 0.28 - 0.034\xi + (0.1\xi)^9$$
$$C_{f0} = 2ce^{-0.391\xi}$$
$$H_0 = 1.251 - 0.0131\xi + 5.35\xi^{-2.85}$$
$$c = 0.001\left[6.55 - 0.0685(\xi - 4.4) + 0.2506(\xi - 4.4)^2\right]$$
$$\xi = \lg R_2, \quad f = \frac{e^{2.6945}U_{z\delta}'}{c\,\mathrm{Re}\,U_{z\delta}^2}$$

# Belotserkovsky's Modeling of
the Memphis Data

Wake Vortex Decay IGE
J.N. Hallock (1975)

■ Hallock reported the elevation and strength of wake vortices of aircraft landing on runway 31R at J. F. Kennedy IA using monostatic acoustic radars.   In addition, the vertical velocity field, translational velocity, and the circulation distribution within the vortex were measured. Effective strength was calculated from the measured vertical velocity distributions.

• Figure shows the circulation distribution for four different B-707 cases (35-50 seconds old). "The effective strength stabilizes between 45 and 70 ft (13.7-21.3 meters).

68
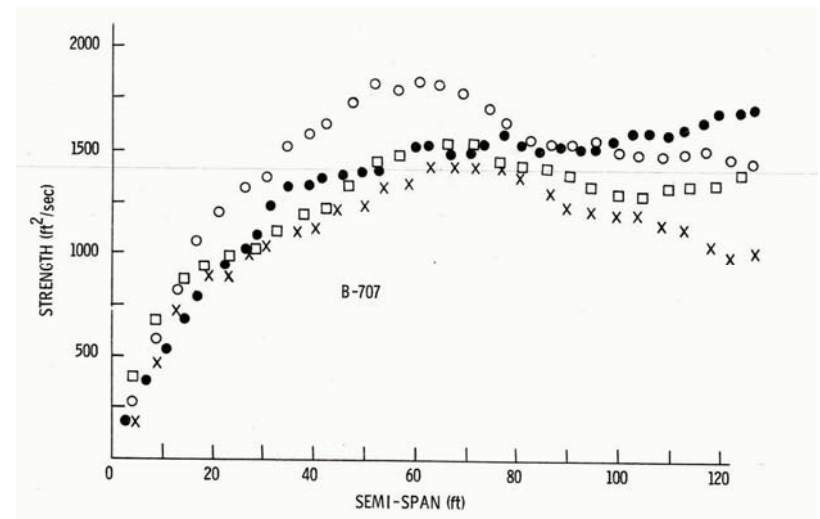
Wake Vortex Decay IGE
J.N. Hallock (1975)
(Continued)

- The figure shows "the very rapid decay" mode of the vortices. This is one of three modes of vortex decay discussed by Hallock.

- "Once the decay commences, the strength is seen to decrease by a factor of two in approximately 15 seconds." It was also observed that (a) the rapid decay commences sooner and occurs more often when the ambient turbulence is high and (b) for a given turbulence level, the larger aircraft begin the rapid decay later than the smaller aircraft. Hallock conjectured that "the rapid decay is caused by a sinusoidal instability in which the vortex has linked with its image vortex."

- As noted earlier, Proctor, Hamilton, & Han (2000) found that ground linking occurs for the eddy dissipation rate larger than 0.3.
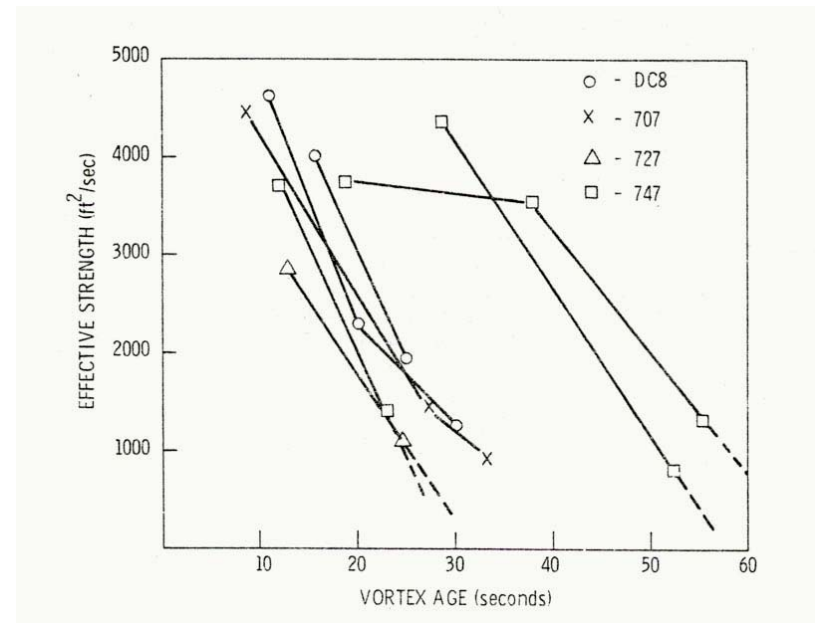
Wake Vortex Decay near the Ground
J.N. Hallock (1975)
(Continued)

- Figure 3 shows one of the three vortex decay modes observed by Hallock near the ground.
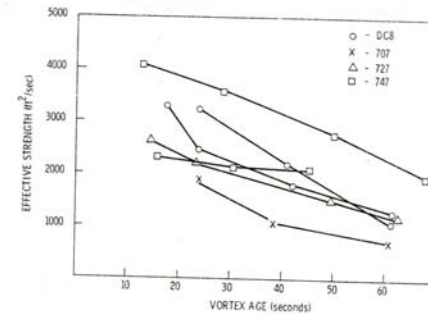He hypothesized that the vortices are decaying through viscous or turbulent diffusion.

Fig. 3: One of the three vortex decay modes near the ground; it is hypothesized that the vortices are decaying through viscous or turbulent diffusion.
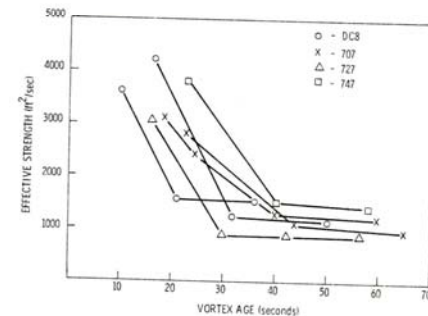
- Figure 4 shows the third mode of decay near the ground. It is assumed that the vortices have experienced a core breakdown leaving behind a remnant with a residual strength of approximately 1000 ft^2/s. Interestingly enough, Hallock noted that "often after a vortex has 'burst' a smaller core becomes discernable as smoke is transported by the axial flow in the vortex from an unburst portion of the remnant."

Fig. 4: One of the three vortex decay modes near the ground; it is hypothesized that the vortices have experienced a core breakdown leaving behind a remnant with a residual strength of approximately 1000 ft^2/sec.

70

Wake Vortex Decay Near the Ground
Under Conditions of Strong Stratification and Wind Shear
Rudis, Burnham, Janota (1996)

• Using the tower fly-by method, decay measurements were made on wake vortices generated by B-727, B-757 and B-767 aircraft. Numerous sensors were used to acquire vortex data.

• Figure 8 shows the normalized circulation decay for B-727 low altitude runs;

• Figure 9 shows the normalized circulation decay for B-757 morning runs; and

• Figure 10 shows the normalized circulation decay for B-767 morning runs.

   The authors have concluded that "Vortices from fly-bys do not simulate the effects of actually landing where the vortices disappear."
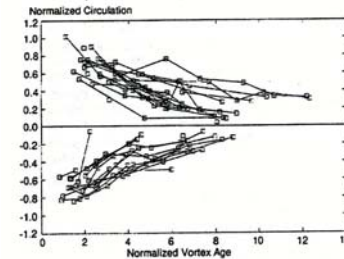
Figure 8. Normalized Circulation Decay for B-727 Low-Altitude Morning Runs
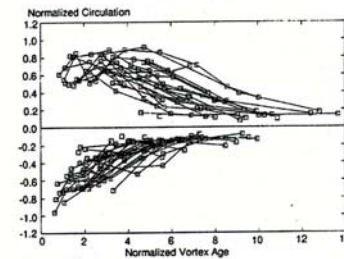
Figure 9. Normalized Circulation Decay for B-757 Morning Runs

• The authors associated the normalized vortex lifetimes (T1 and T2) with selected atmospheric variables for the purpose of possibly identifying statistical relationships. Figures contain data from all three aircraft, include linear regression lines and present the regression equations (at the top of plots).

• Figure 18 (top) is a plot of T1 and T2 versus the adjusted crosswind shear at 30 m.

• Figure 19 is a plot of T1 and T2 versus the normalized wind speed at 30 m.

• The authors concluded that data from operational settings are needed to assess the effects of vortex termination on vortex decay at locations up the glideslope.
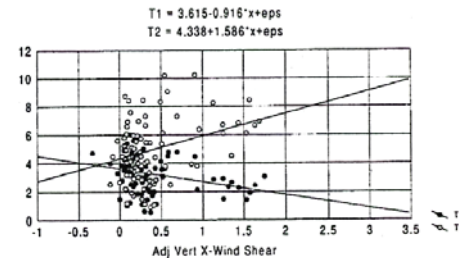
Figure 18. Normalized T1 and T2 vs. Adjusted Crosswind Shear at 30 m

6.3 Windspeed

Windspeed itself should be a factor in vortex lifetime in the sense that stronger winds are generally associated with stronger turbulence; therefore, if turbulence is predicted by windspeed, both T1 and T2 should decrease with increasing windspeed. Figure 19 plots T1 and T2 against non-dimensional windspeed at 30 m. The regressions lines for both T1 and T2 indicate a general tendency for the longer lifetimes to occur for lower windspeeds and vice versa.
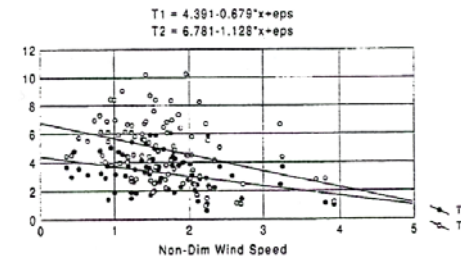

Figure 19. Normalized T1 and T2 vs. Non-Dimensional Wind Speed at 30 m

Measurements of Wake Vortices Interacting the Ground
Burnham & Hallock (1998)
(Continued)

- Burnham and Hallock (1998) augmented a propeller anemometer array with a sonic anemometer measuring 3-D wind and temperature at 10 Hz, and a vertical array of vertical wind and crosswind anemometers. In general, in low to moderate turbulence, the turbulence level inside the the wake vortex flow field was found to be greater than that in the ambient wind. The vertical array showed that the crosswind profile under a wake vortex IGE has a very thin boundary layer, much thinner than that of the ambient wind.

- In addition, they devised a vortex-pair model by assuming that the vortices do not decay, fluid slips along the wall and the real boundary layer may be ignored. They have noted: "nevertheless, the image model gives a first order approximation..." and obtained the plots shown on the right.   Clearly, such representations do not constitute even a first order approximation and have nothing to do with the reality or the rebound.
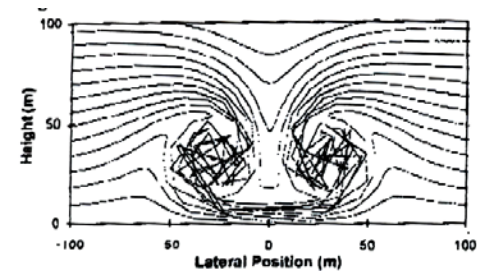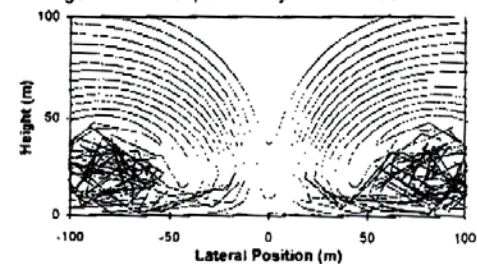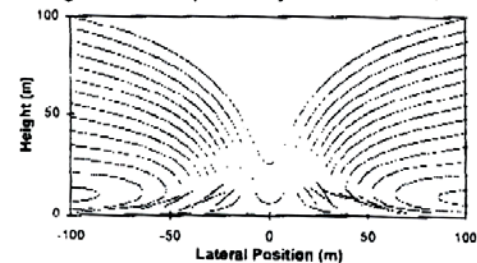

Figure 1. Atmospheric Layers at 12 Seconds

Figure 2. Atmospheric Layers at 50 Seconds

Wake Turbulence Limits on Paired Approaches to Parallel Runways
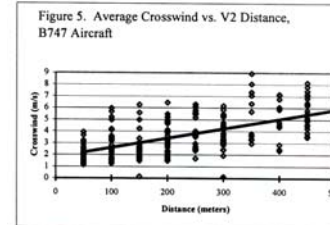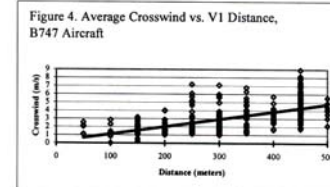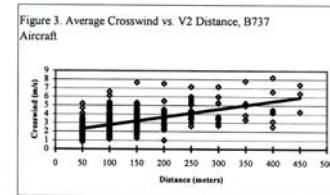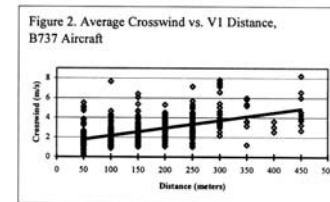## Burnham, Hallock, & Greene (2002)

- Burnham, Hallock, and Green (2002) assessed, from an operational point of view, the tradeoffs between longitudinal spacing and crosswind, needed to prevent wake encounters, by modeling and by examining the existing wake lateral transport data from two airports at distances of 1500-3000 ft from the runway threshold. Figure shows the speed differential (vortex transport and the ambient cross wind) as a function of travel time.

- They have concluded that:

- (1) runways separated by no more than 1000 ft will permit longitudinal pair separation of not much greater than 20 s (no cross wind); and

- (2) for runways separated by about 600 ft, the allowed crosswinds will reduce to 4 kn and the aircraft separation will have to be increased.
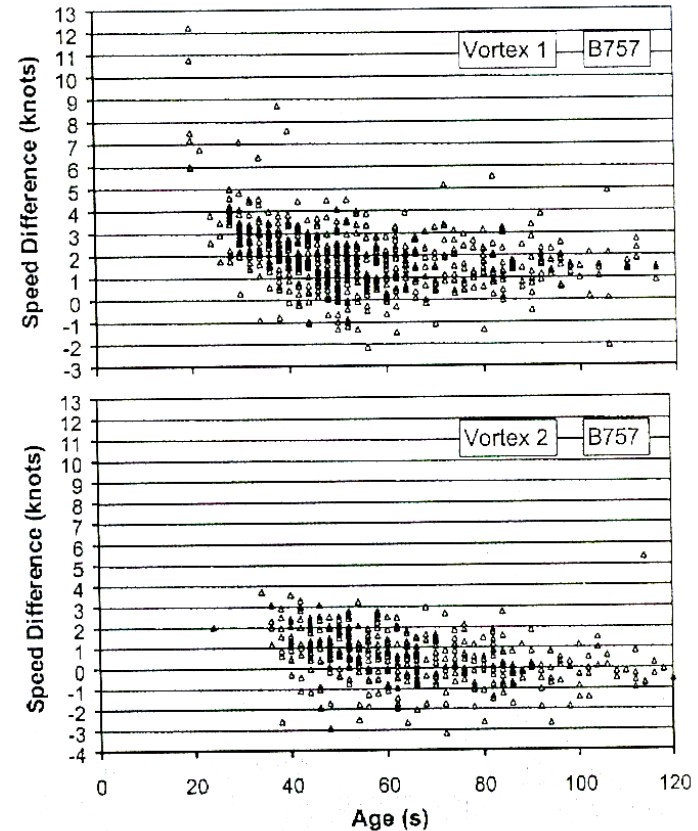
Wake Vortex Effects on Parallel Runway Operations
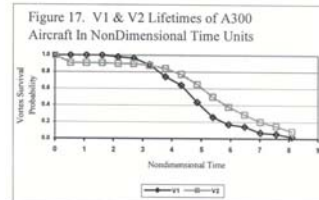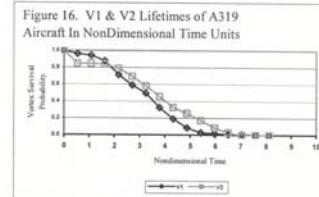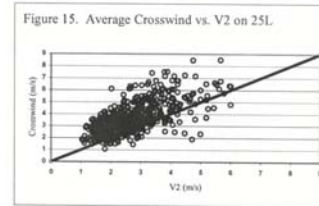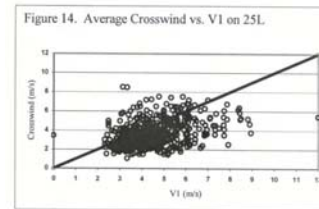## Hallock, Osgood, Konopka (2003)

- Hallock, Osgood, and Konopka (2003) studied the aircraft wake vortex behavior in ground effect between two parallel runways at Frankfurt/Main in terms of the crosswind, aircraft type, and a measure of atmospheric turbulence. The plots show the distances the vortices translated as a function of 1-minute average crosswind (B-737 & B-747). The solid line is a least-squares fit to the data.

- The only conclusion that can be reached is that the downwind vortex (V1) travels, as may be expected, farther than the upwind vortex (V2) for a given crosswind. The authors have also concluded that vortex decay in ground effect is little influenced by ambient turbulence and is seen to be a stochastic process.

Figure 2. Average Crosswind vs. V1 Distance, B737 Aircraft

Figure 3. Average Crosswind vs. V2 Distance, B737 Aircraft

Figure 4. Average Crosswind vs. V1 Distance, B747 Aircraft

Figure 5. Average Crosswind vs. V2 Distance, B747 Aircraft

Wake Vortex Effects on Parallel Runway Operations
## Hallock, Osgood, Konopka (2003) (Continued)

- The two to figures indicate that V1 (downwind vortex) was about 1 m/s faster and V2 was about 1 m/s slower than the crosswind. Many of the cases which have shown the opposite trend were for short-lived vortices.

- Figures 16 & 17 (the bottom two) show the vortex lifetimes for A-319 and A-300 in normalized units (one unit is approximately 18 s for both types of aircraft).

- The dip at about 1/2 unit for non-dimensional time for V2 is caused by the minimum 1 m/s crosswind restriction. Consequently, about 10% of the landings did not record a V2 vortex.

Figure 14. Average Crosswind vs. V1 on 25L

Figure 15. Average Crosswind vs. V2 on 25L

Figure 16. V1 & V2 Lifetimes of A319 Aircraft In NonDimensional Time Units

Figure 17. V1 & V2 Lifetimes of A300 Aircraft In NonDimensional Time Units

Wake Vortex Effects on Parallel Runway Operations
Hallock, Osgood, Konopka (2003) (Continued)

- Based on about 2,500 landings in April 1998, five effects were established that affect how the capacity of parallel runways might be increased:

- V1 (downwind) decays faster than V2;

- The distance the vortices move is dependent on the crosswind magnitude;

- Ambient turbulence is shown to play a lesser role in the demise of vortices IGE;

- Temperature measurements near a suspected vortex might lead to a dependable means to distinguish a vortex from a wind gust; and

- One can make a reasonable estimate of the vortex behavior for aircraft not included in original tests shown in Figure on the basis of the data so far obtained with a Learjet 35, up to B-747-400.

Figure 18. Vortex Lifetimes vs. Maximum Landing Weight
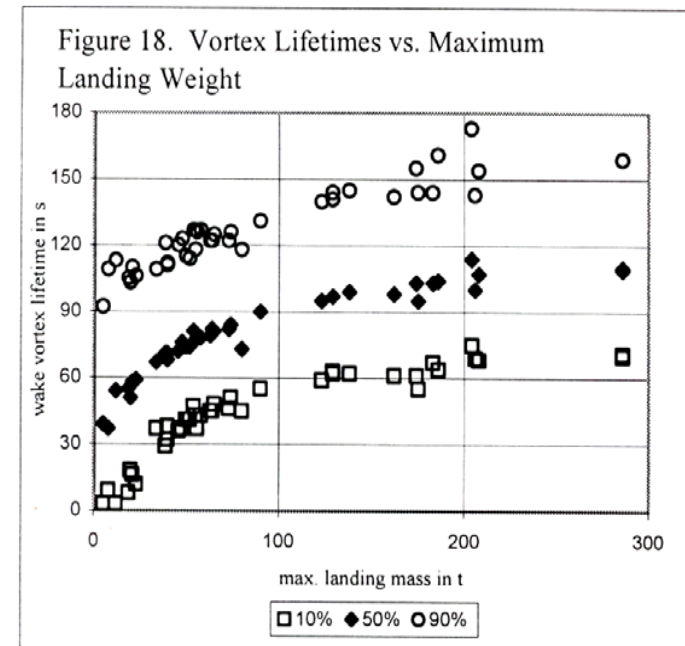
Summary

the requirement is:

Devising of physics-based parametric models for the prediction of (operational) real-time response, mindful of the highly three-dimensional and unsteady structure of vortices, boundary layers, atmospheric thermodynamics, and weather convective phenomena.

- It is not sufficient to bring large amounts of plots and data before one's attention span. It is necessary to bring physical 'insight' into that span in terms of the fundamental principles of physics, fluid mechanics, numerical analysis, and heuristic reasoning. Unsubstantiated, exaggerated claims lead to erroneous conclusions and become an impediment to further progress. Thus, it is important to discuss the shortcomings more, and the virtues less, of any model.

- The development of models for the IGE which consider the most important parameters of the vortices, the ground, and the environment, with as few robust constants as possible, is indeed a very difficult task. It is this difficulty that led to 'mimicking' in lieu of 'modeling.'

- We define a model as

"A robust real time predictor based on physics, numerical simulations (LES), field data (covering a large parameter space) and heuristic reasoning." It should not violate the equations of motion or avoid fundamental boundary conditions like no slip, no penetration. It should not violate the fundamental laws of mechanics. It should not be too sensitive to any one parameter.

Finally, it should work in the field!

Summary
(Continued)

- **At present**:

- There is considerable data, obtained with representative types of aircraft.

- There are highly-idealized theoretical solutions (some with imbedded unacceptable assumptions).

- There are algorithms that "mimic" IGE (with very little physics);

- There are numerous <u>laminar-flow</u> calculations (with no wind and/or shear) which cannot be used as an operational real-time-response tool (low Re, and too much CPU);

- There are several numerical solutions at high Re (<u>laminar solutions,</u> mimicking turbulence with <u>constant viscosity</u> or artificial dissipation);

- There are a few numerical calculations based on particle methods with Re based on a <u>constant viscosity</u> (with too many, and often arbitrary, schemes).

- There are LES solutions at fairly high Re (in need of inclusion of shear, etc.) <u>on which models may be based;</u>

- Only a few of the above efforts give a hint as to how the results can be used to <u>create a model</u>;

- What is needed is <u>an operational, physics based model with only a few data-fitted parameters</u>!

Summary
(Continued)

In creating a MODEL, LES and Field data will be the most powerful tools.

- Models that cannot deal with highly unsteady boundary layers, separation and shedding of vorticity in lumps, turbulence, the complexities of the creation, rapid convection and diffusion of vorticity without introducing numerous schemes are not likely to contribute to future progress.

- One must be mindful of the highly three-dimensional and unsteady structure of vortices, turbulent boundary layers, atmospheric thermodynamics, and weather convective phenomena.

- **Windline data** do not appear to be of great help to a model creation. To use it one should already have an accurate model which **correctly predicts** where the vortices (and the windline) will be before they appear as windlines! The reverse solution may yield some results under highly clean conditions (no stratification, no shear (but wind), no strong ambient turbulence, etc.). The acquisition of the windline data may be pursued with the belief that it will help to solve the wake encounter problems at parallel airports while awaiting for a MODEL!

Summary

- It is not yet clear if and how the windline data (often averaged & often obtained at relatively small heights) can be used for the analysis and verification of the vertical and lateral positions of the vortices and their strengths in an environment with wind/shear, stratification, ground, ground-linking, and intense turbulence. One must note the fact that in the ground effect region the gradients of practically every major parameter are very strong and their correct prediction is at present beyond the power of the existing models.

- 2-D TASS simulation by Dr. Proctor shows the positions of vortices in a wind/shear environment (at ≈ 65 ft and 100 ft). The question is: Where are the vortex cores when the wind line sensors are a mere 3 feet off the ground (as in SFO)?
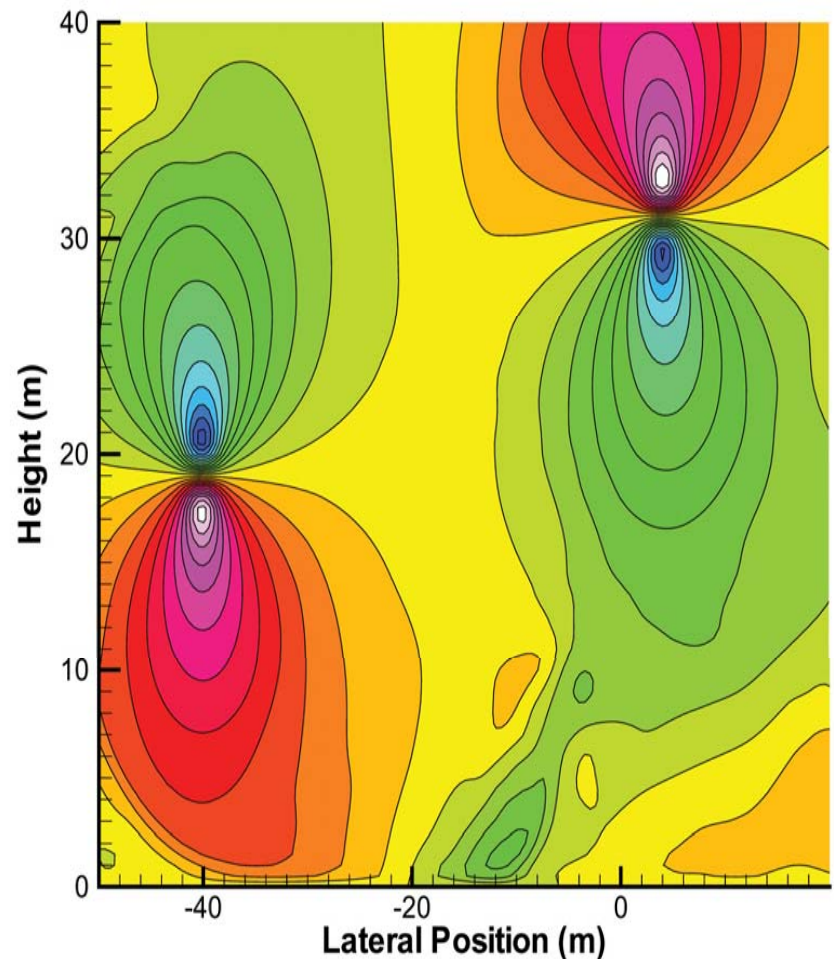
E N D

Prepared by:

Dist. Prof. Turgut 'Sarp' Sarpkaya

Dept. of Mechanical & Astronautical Engineering

Naval Postgraduate School

Monterey, CA 93943

E-mail: sarp@nps.edu

Fax: (831)-656-3425